

NaPiIIb Expression and Intestinal Phosphate Absorption are Increased in Young Mice

by

Tate MacDonald

A thesis submitted in partial fulfillment of the requirements for the degree of

Master of Science

Department of Physiology

University of Alberta

© Tate MacDonald, 2022

ABSTRACT

Phosphate is important for a variety of physiological functions, including the composition of bone via formation of the calcium-phosphate salt hydroxyapatite. Given that bone mineralization occurs very rapidly early in life, young mammals require high phosphate absorption to establish and maintain the required phosphate balance for the high rate of bone mineralization. Absorption of all ions including phosphate from the small intestine takes place via either the active transcellular or passive paracellular pathway. A key player in the former pathway is NaPiIIb; a secondary active sodium-phosphate transporter expressed at the apical membrane of enterocytes. Conversely, claudins are a family of proteins expressed in the tight junction that govern the paracellular passage of specific ions. Failure to establish adequate phosphate balance often results in diminished bone integrity. This work sought to establish the relative importance of the two pathways of ion absorption in the upregulation of phosphate absorption in young animals. To accomplish this, ontogenic changes in expression of genes involved transcellular and paracellular phosphate absorption in mice were assessed between one day and six months of age. Additionally, functional differences in phosphate absorption via the two pathways of absorption were assessed in pre-weaning juvenile mice and adult mice. NaPiIIb message levels were consistently elevated along the length of the small intestine in juvenile mice. Accordingly, net transcellular phosphate flux assessed *ex vivo* was increased in juvenile mice relative to adult counterparts. NaPiIIb was specifically implicated in this increase by administering the NaPiIIb inhibitor NTX-1942 which attenuated the increased apical-to-basolateral phosphate absorption observed in young mice. Further, the expression of two claudins hypothesized to be involved in paracellular phosphate absorption; claudins -4 and -23;

were upregulated early in murine development. Consistent with this, paracellular phosphate permeability was increased along the length of the small intestine in young mice relative to adults. The findings of this study are consistent with young mice increasing phosphate absorption via both the transcellular and paracellular pathway to the end of establishing a sufficiently high phosphate balance for normal bone mineralization.

PREFACE

This thesis is a part of a project; The role of transport proteins in Epithelial Sodium, Bicarbonate, Phosphate and Calcium Transport and Breeding Colonies, AUP00000213, which has received research ethics approval from the University of Alberta Research Ethics board.

A review of many of the items outlined in Chapter 1 of this thesis was published as **MacDonald T, Saurette M, Beggs MR and Alexander RT**. Developmental Changes in Phosphate Homeostasis. *Rev Physiol Biochem Pharmacol* 179: 117-138, 2021.

ACKNOWLEDGEMENTS

Firstly, I would like to thank my fellow trainees of this laboratory, past and present, for the support you have provided me throughout my studies. Among the trainees I owe my thanks to are Megan Beggs, Rebecca Tan, Kennedy Young, Harneet Bhullar, Matthew Saurette and Justin Lee. I am also extremely grateful for the guidance provided by our laboratory technicians, Debbie O'Neill and Wanling Pan. Without the technical expertise you shared with me, the success of my graduate work would not have been possible. Further, I would like to extend my deepest gratitude to my supervisor, Dr. Todd Alexander, who has created an environment that truly brings the best out of trainees and technicians. Your leadership style has allowed the members of this lab, myself included, to develop and flourish as researchers.

Beyond members of my immediate laboratory, I would like to offer my sincere thanks to the members of my committee, Dr. Kyla Smith and Dr. Emmanuelle Cordat, for lending me your wealth of experience and expertise in guiding my project to its successful completion. Also sitting on my committee is my supervisor Dr. Todd Alexander, to whom I extend further thanks for your extensive guidance as well as your assistance in the selection of faculty researchers I am truly proud to call my committee members.

I would also like to thank the Natural Sciences and Engineering Research Council of Canada for their financial support during my studies.

Lastly, I extend my gratitude to my friends and family for their invaluable and multifaceted support during my studies. To say the least, the task of completing my work during the COVID-19 pandemic would have been extraordinarily difficult without you.

TABLE OF CONTENTS

CHAPTER 1: INTRODUCTION	1
PHOSPHATE AND ITS PHYSIOLOGICAL FUNCTIONS	2
PHOSPHATE HOMEOSTASIS OVERVIEW	2
DIETARY PHOSPHATE SOURCES, BIOAVAILABILITY, AND IMPLICATIONS FOR ABSORPTION	4
CAUSES AND CONSEQUENCES OF ALTERED PHOSPHATE HOMEOSTASIS	9
PHOSPHATE HANDLING IN THE DEVELOPING MAMMAL	11
INTESTINAL PHOSPHATE ABSORPTION AND RENAL PHOSPHATE REABSORPTION – THE TRANSCELLULAR PATHWAY	11
NAPIIIA	11
NAPIIIB	12
NAPIIIC	14
PIT1	15
PIT2	16
PATHWAYS OF PHOSPHATE ABSORPTION – THE PARACELLULAR PATHWAY	17
PARACELLULAR PHOSPHATE ABSORPTION – THE ROLE OF CLAUDINS	17
INTESTINAL PHOSPHATE ABSORPTION – ALKALINE PHOSPHATASE	23
DEVELOPMENTAL CHANGES IN INTESTINAL PHOSPHATE HOMEOSTASIS	24
DEVELOPMENTAL CHANGES IN RENAL PHOSPHATE HOMEOSTASIS	25
RATIONALE AND HYPOTHESIS	25
CHAPTER 2: MATERIALS AND METHODS	27
ETHICS APPROVAL AND ANIMALS	28
ISOLATION OF BIOLOGICAL SAMPLES	28
REAL-TIME POLYMERASE CHAIN REACTION	28
BLOOD AND URINE BIOCHEMISTRY	30
USSING EXPERIMENTS – TISSUE PREPARATION AND MOUNTING	30
DETERMINATION OF PARACELLULAR PHOSPHATE PERMEABILITY – BI-IONIC DIFFUSION POTENTIALS	31
DETERMINATION OF NET TRANSCELLULAR PHOSPHATE FLUX	33
INHIBITION OF NAPIIIB IN JUVENILE APICAL TO BASOLATERAL FLUX	35
STATISTICAL ANALYSIS	36
CHAPTER 3: RESULTS	38
BLOOD AND URINE PHOSPHATE LEVELS AT DIFFERENT AGES	39
CHANGES IN GENE EXPRESSION OF THE TRANSCELLULAR PATHWAY AT DIFFERENT DEVELOPMENTAL AGES IN THE KIDNEY	41
DESPITE SIGNIFICANTLY INCREASED NAPIIIB EXPRESSION AT P7 AND P14 IN THE DUODENUM, THERE IS NOT INCREASED NET PHOSPHATE FLUX	43
SIGNIFICANTLY INCREASED NAPIIIB EXPRESSION BEFORE P14 IN THE JEJUNUM CONFERS INCREASED NET PHOSPHATE FLUX	45
SIGNIFICANTLY INCREASED NAPIIIB EXPRESSION AT P14 IN THE ILEUM CONFERS INCREASED NET PHOSPHATE FLUX	47
PARACELLULAR PATHWAY GENE EXPRESSION AND PERMEABILITY ACROSS DEVELOPMENT IN THE DUODENUM	49

PARACELLULAR PATHWAY GENE EXPRESSION AND PERMEABILITY ACROSS DEVELOPMENT IN THE JEJUNUM	51
PARACELLULAR PATHWAY GENE EXPRESSION AND PERMEABILITY ACROSS DEVELOPMENT IN THE ILEUM	53
CHAPTER 4 – DISCUSSION	61
<hr/>	
INTESTINAL PHOSPHATE ABSORPTION IN THE YOUNG MOUSE – IMPORTANCE OF THE TRANSCELLULAR AND PARACELLULAR PATHWAY	62
PHOSPHATE ABSORPTION IN THE JUVENILE ANIMAL - A PROPOSED MODEL	63
PHOSPHATE ABSORPTION IN THE ADULT ANIMAL - A PROPOSED MODEL	66
FUTURE DIRECTIONS	69

LIST OF TABLES

TABLE 1.1 GENETIC CAUSES OF HYPOPHOSPHATEMIA.	10
TABLE 2.1. PRIMER AND PROBE SEQUENCES FOR RT-PCR.	30
TABLE 2.2. IONIC COMPOSITION OF BUFFERS USED IN BI-IONIC DIFFUSION POTENTIAL EXPERIMENTS.	37

LIST OF FIGURES

FIGURE 1.1. LUMEN PH ALONG THE LENGTH OF THE SMALL INTESTINE.	5
FIGURE 1.2. REGULATORY POINTS IN PHOSPHATE HOMEOSTASIS.	6
FIGURE 1.3. PHOSPHATE REABSORPTION FROM THE RENAL TUBULE.	7
FIGURE 1.4. ENDOCRINE REGULATION OF PHOSPHATE HOMEOSTASIS.	8
FIGURE 1.5. RENAL PHOSPHATE REABSORPTION IN THE PROXIMAL TUBULE.	20
FIGURE 1.6. PHOSPHATE ABSORPTION IN THE SMALL INTESTINE.	21
FIGURE 1.7. GENERAL CLAUDIN TERTIARY STRUCTURE.	21
FIGURE 1.8. THE CLAUDIN-23 GENOMIC REGION.	22
FIGURE 3.1. SERUM AND URINE BIOCHEMISTRY IN JUVENILE AND ADULT MICE.	40
FIGURE 3.2 DEVELOPMENTAL CHANGES IN TRANSPORTERS INVOLVED IN TRANSCELLULAR RENAL PHOSPHATE REABSORPTION.	42
FIGURE 3.3 EXPRESSION AND FUNCTION OF THE TRANSCELLULAR PHOSPHATE TRANSPORT PATHWAY IN THE DUODENUM.	44
FIGURE 3.4. EXPRESSION AND FUNCTION OF THE TRANSCELLULAR PHOSPHATE TRANSPORT PATHWAY IN THE JEJUNUM.	46
FIGURE 3.5. EXPRESSION AND FUNCTION OF THE TRANSCELLULAR PHOSPHATE TRANSPORT PATHWAY IN THE ILEUM.	48
FIGURE 3.6 GENE EXPRESSION PROFILE AND FUNCTIONAL DIFFERENCES IN PARACELLULAR PHOSPHATE PERMEABILITY ACROSS DEVELOPMENT IN THE DUODENUM.	50
FIGURE 3.7 GENE EXPRESSION PROFILE AND FUNCTIONAL DIFFERENCES IN PARACELLULAR PHOSPHATE PERMEABILITY ACROSS DEVELOPMENT IN THE JEJUNUM.	52
FIGURE 3.8. GENE EXPRESSION PROFILE AND FUNCTIONAL DIFFERENCES IN PARACELLULAR PHOSPHATE PERMEABILITY ACROSS DEVELOPMENT IN THE ILEUM.	54
FIGURE 3.9. NAPIIIB EXPRESSION IN ALL ASSESSED AGES AND SMALL BOWEL SEGMENTS.	56
FIGURE 3.10. PIT1 EXPRESSION IN ALL AGES AND ALL SMALL BOWEL SEGMENTS.	56
FIGURE 3.11. PIT2 ABUNDANCE IN ALL ASSESSED AGES AND SMALL INTESTINE SEGMENTS.	57
FIGURE 3.12. INTESTINAL ALKALINE PHOSPHATASE ABUNDANCE IN ALL STUDIED AGES AND SMALL BOWEL SEGMENTS.	57
FIGURE 3.13. ABUNDANCE OF MESSENGER RNA ENCODING THE VITAMIN D RECEPTOR ACROSS ALL AGES AND SMALL BOWEL SEGMENTS	58
FIGURE 3.14. ABUNDANCE OF CLAUDIN-3 MESSENGER RNA LEVEL AT ALL ASSESSED AGES AND SMALL BOWEL SEGMENTS.	58
FIGURE 3.15. CLAUDIN-4 MESSENGER RNA LEVELS IN ALL ANALYZED AGES AND SMALL INTESTINE SEGMENTS. MRNA ABUNDANCE NORMALIZED TO GAPDH.	59
FIGURE 3.16. CLAUDIN-7 MESSAGE ABUNDANCE ACROSS DEVELOPMENT IN ALL SMALL BOWEL SEGMENTS.	59
FIGURE 3.17. ABUNDANCE OF MESSENGER RNA ENCODING CLAUDIN-23 ACROSS DEVELOPMENT AT EACH SMALL INTESTINE SEGMENT.	60
FIGURE 4.1. A PROPOSED MODEL OF INTESTINAL PHOSPHATE HOMEOSTASIS IN JUVENILE AND ADULT MICE.	68

LIST OF ABBREVIATIONS

ADP	Adenosine diphosphate
AMP	Adenosine monophosphate
ATP	Adenosine triphosphate
BBMV	Brush border membrane vesicles
CKD	Chronic kidney disease
Cldnd-1	Claudin domain-containing protein 1
ddH ₂ O	Double-distilled water
FAM	Fluorescein labeled amidite reporter dye
FGF23	Fibroblast growth factor 23
FVB/N	Friend leukemia virus B; N strain-sensitive
GAPDH	Glyceraldehyde 3-phosphate dehydrogenase
HHRH	Hereditary hypophosphatemic rickets with hypercalciuria
iALP	Intestinal alkaline phosphatase
NaPiIIa	Sodium-dependent phosphate transporter type IIa
NaPiIIb	Sodium-dependent phosphate transporter type IIb
NaPiIIc	Sodium-dependent phosphate transporter type IIc
NFQ-MGB	Nonfluorescent quencher-minor groove binder
NHE3	Sodium-hydrogen exchanger type 3
PHEX	Phosphate regulating endopeptidase homolog X-linked
Pit1	Sodium-phosphate transporter 1
Pit2	Sodium-phosphate transporter 2
PTH	Parathyroid hormone

P-33	Phosphorus 33
RT-PCR	Real-time PCR
RXR	Retinoid X receptor
TEER	Transepithelial electrochemical resistance
TTX	Tetrodotoxin
VDR	Vitamin D receptor
VIC	Victoria reporter dye
Vmax	Velocity maximum of substrate binding-to-release
XLHR	X-linked hypophosphatemic rickets

Chapter 1: Introduction

Phosphate and its Physiological Functions

Phosphate is a multivalent ion that performs a wide variety of roles in the body. These roles include contributing to the composition of the phospholipid bilayer that forms cell membranes, energy currency in the form of nucleotide phosphates, ATP, ADP, cyclic AMP, and contributing to the composition of the calcium-phosphate salt hydroxyapatite ((Ca)₁₀(PO₄)₆(OH)₂) in the extracellular matrix of bone tissue. Phosphate is a multivalent ion with four protonation states (H₃PO₄, H₂PO₄⁻, HPO₄²⁻, PO₄³⁻) and three pKa values of approximately 2.2, 7.2, and 12.7 (1). The protonation state phosphate occupies is dictated by the local pH. Of note, the pH of the small intestine varies from acidic in the proximal segment to alkaline in the mid to distal small bowel (2) (*Figure 1.1*). Accordingly, the predominant phosphate species is monovalent in the duodenum, and divalent in the jejunum and ileum. In healthy humans, serum phosphate is tightly regulated within the normal clinical range of 0.8 -1.5 mM. Serum phosphate in infants is slightly higher than this range and declines across development to adult values (3, 4). However, it should be noted that serum phosphate levels are low at birth and increase markedly between birth and 1 month of age to the high levels observed in infancy (4). Approximately 10% of serum Pi is protein-bound, another 5% is bound to cations in the blood, and the remaining 85% is unbound (5). The intracellular phosphate concentration is reported to exceed 100 mM (6).

Phosphate Homeostasis Overview

The general physiological processes regulating phosphate homeostasis are absorption from the small intestine, deposition and resorption to and from bone, and reabsorption from the renal ultrafiltrate upon filtration at the glomerulus (*Figure 1.2, Figure 1.3*). The small intestine is

divided into the duodenum, jejunum, and ileum from proximal to distal. At each point of regulation, phosphate homeostasis is subject to hormonal control. For instance, upon an increase in serum phosphate, parathyroid hormone (PTH) is released from the parathyroid gland. PTH induces a modest degree of resorption of phosphate from bone, but its primary phosphotropic effect is the induction of phosphaturia by reducing phosphate reabsorption from the renal ultrafiltrate. The net effect of PTH release is therefore to restore serum phosphate to appropriate levels via urinary phosphate losses. In addition, PTH promotes the synthesis of the active form of vitamin D; 1,25 (OH)₂ Vitamin D₃ (calcitriol). Calcitriol in turn increases the production of fibroblast growth factor 23 (FGF23), which, similarly to PTH, induces phosphaturia by decreasing phosphate reabsorption (*Figure 1.4*). Calcitriol also increases the absorption of phosphate and calcium (Ca²⁺) from the small intestine. While PTH and FGF23 have similar effects in restoring serum phosphate to normal levels via increasing phosphate losses, it appears that PTH functions on a more immediate time scale (minutes/hours) in comparison to FGF23 (days/weeks) (7, 8). It should be noted that while PTH regulates FGF23 expression, phosphate may independently increase FGF23 abundance; likely through the receptor FGFR1 (9).

Of note, calcitriol is a remarkably multifaceted compound that regulates many genes. To do so, it binds to the nuclear vitamin D receptor (VDR) which interacts with the retinoid X receptor (frequently abbreviated to RXR) to form a transcription complex. The complex subsequently interacts with a DNA response element upstream of the coding region of the given gene whereupon the VDR acts as a transcription factor. In the context of phosphate homeostasis, calcitriol up-regulates absorption of phosphate from the small intestine, likely via the transcellular pathway (10, 11). Specifically, its putative role in regulating phosphate absorption is upregulation of NaPiIIb expression. Its mode of regulation appears to be age specific.

However, there is evidence that calcitriol may upregulate NaPiIIb at the transcriptional level in young animals, whereas calcitriol-driven NaPiIIb upregulation in adults may occur at the translational level (11).

Dietary Phosphate Sources, Bioavailability, and Implications for Absorption

The sources of dietary phosphate can be broadly classified into two categories; organic and inorganic. Organic phosphorus is generally found in plant and animal foods such as meat, nuts, and leafy greens. Structurally, what distinguishes organic phosphorus is the presence of a carbon-containing R-group to which one or more oxygen atoms in phosphate are covalently linked when ingested. To be clear, when bound to an R-group, dietary phosphate is referred to as organic phosphorus as it is not yet ionized. Depending on the food source, the identity of the R-group may be a lipid, nucleic acid, peptide, or sugar. Prior to absorption, organic phosphorus must be cleaved from the R-group by intestinal alkaline phosphatase (iALP). It is worth noting that in many plant-based foods, organic phosphorus is bound in the form of phytic acid. As humans do not express the phytase enzyme required to liberate phosphate from phytic acid, phosphate derived from this source is more poorly absorbed than that of other organic phosphorus-containing foods (12).

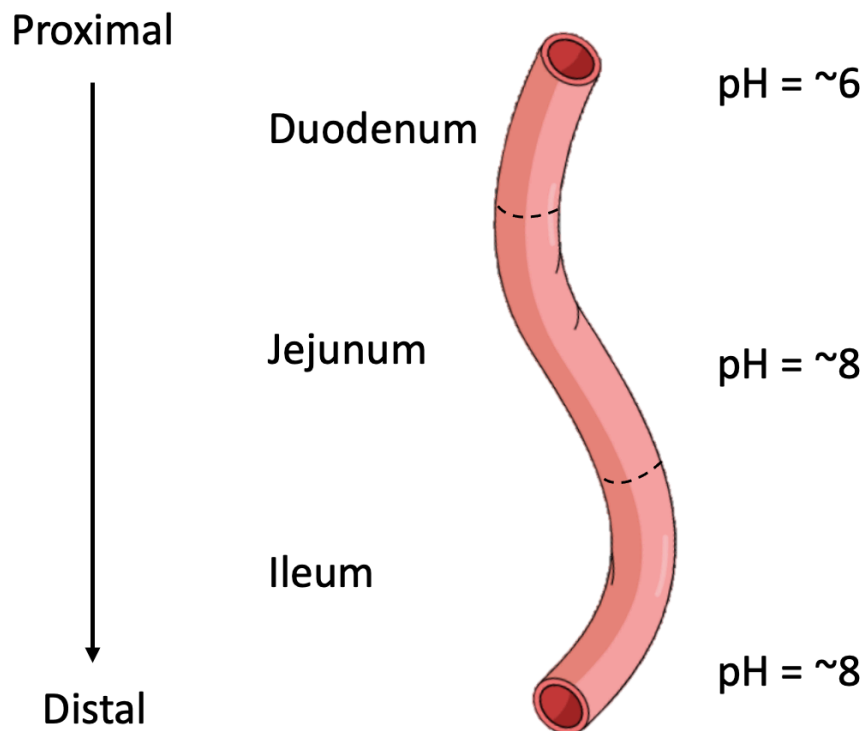


Figure 1.1. Lumen pH along the length of the small intestine. Under normal conditions, the luminal pH is mildly acidic in the duodenum and alkaline in the jejunum and ileum. Since phosphate is a multivalent ion, whose valence is influenced by local pH conditions, the proximal to distal variability in pH will determine the predominant charged state of phosphate.

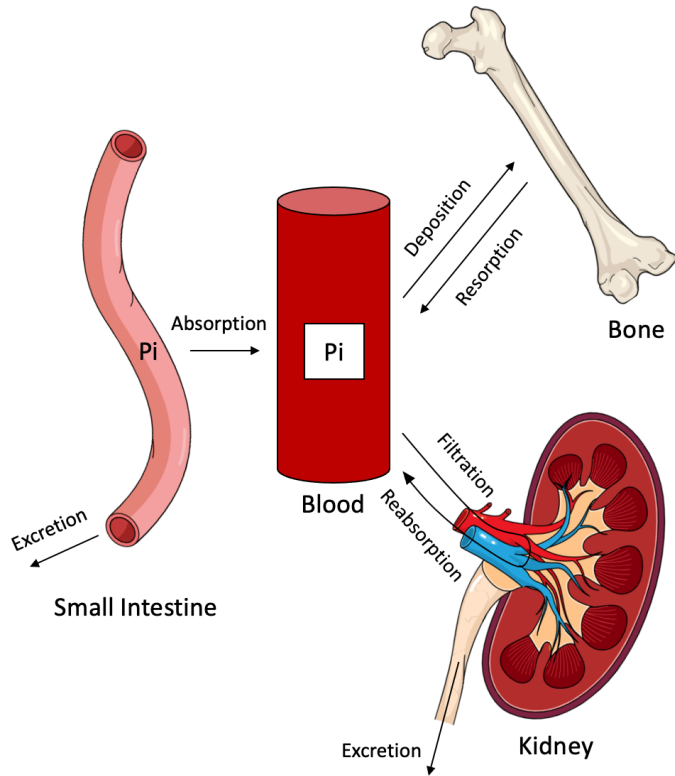


Figure 1.2. Regulatory points in phosphate homeostasis. Upon ingestion, phosphate is either absorbed from the gastrointestinal tract or excreted in the feces. Phosphate in the blood can be mineralized into bone via deposition. Phosphate may also enter the blood from bone via resorption. Free circulating phosphate is filtered through glomeruli in the kidney, whereupon it is either reabsorbed from the tubular lumen of the nephron back into systemic circulation or excreted in the urine.

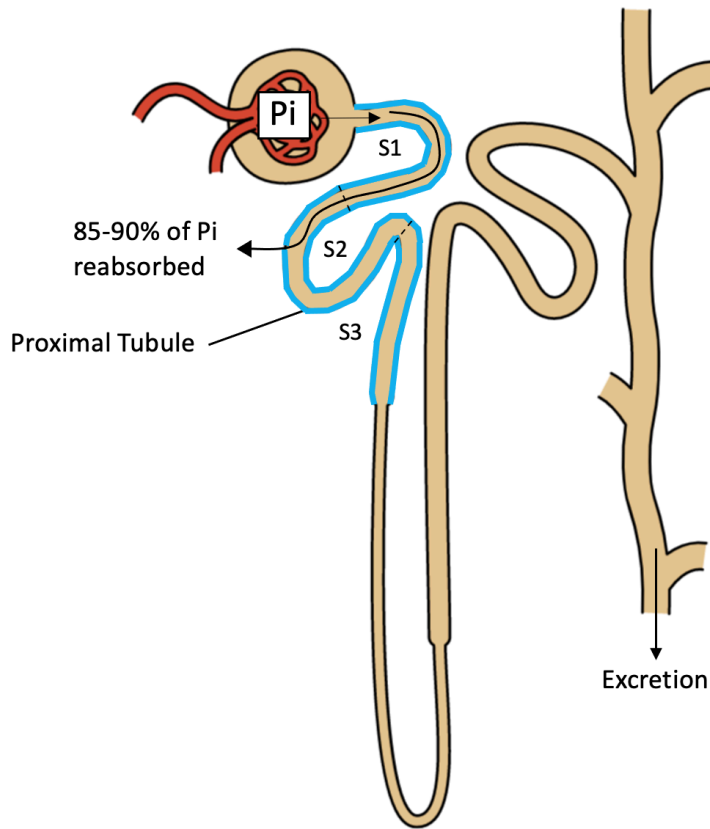


Figure 1.3. Phosphate reabsorption from the renal tubule. Upon filtration at the glomerulus into the tubule lumen, 85-90% of phosphate is reabsorbed from the proximal tubule (blue), which is subdivided into the proximal convoluted tubule (S1, S2) and the proximal straight tubule (S3). NaPiIIa expression decreases along the length of the proximal tubule. The specific distribution profile of NaPiIIc along the proximal tubule is not known. As there is currently a paucity of evidence for phosphate reabsorption in other segments of the nephron, what is not reabsorbed from the proximal tubule is proposed to be excreted in the urine.

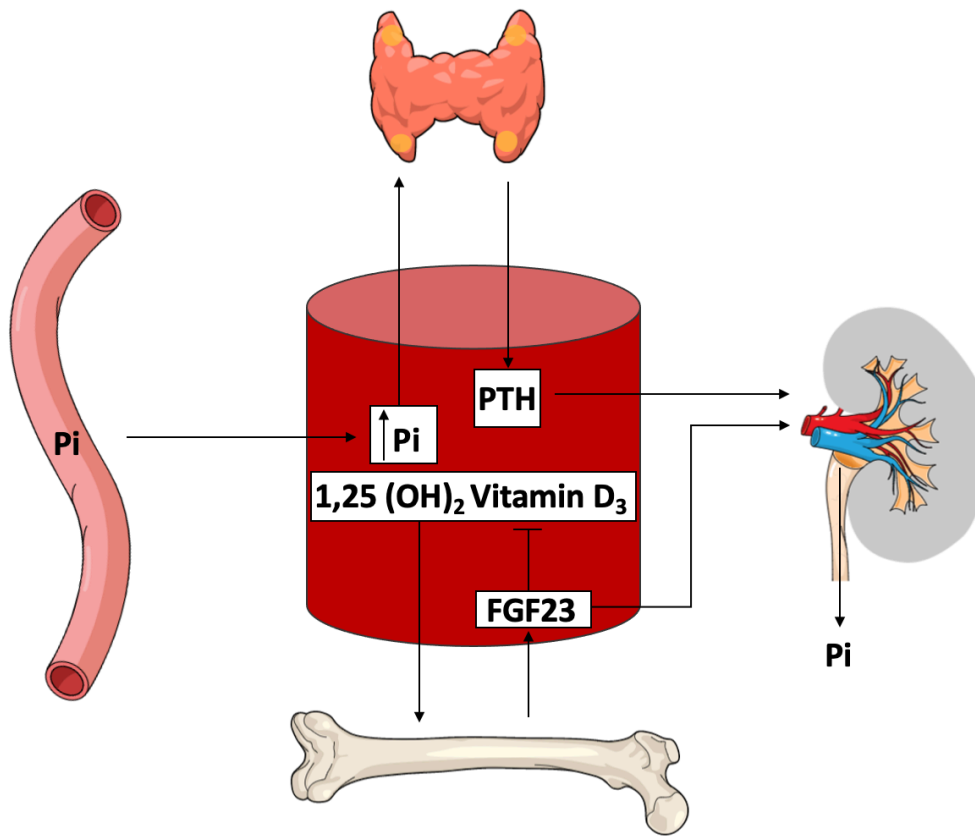


Figure 1.4. Endocrine regulation of phosphate homeostasis. Following absorption of phosphate from the diet, the parathyroid gland senses an increase in serum [phosphate] and increases secretion of PTH. The effect of PTH is twofold: Firstly, PTH has the direct effect of decreasing phosphate reabsorption in the kidney. Secondly, PTH increases synthesis of 1,25 (OH)₂ Vitamin D₃ (calcitriol), which in turn increases the production and subsequent secretion of FGF23 from bone. Similar to PTH, FGF23 increases phosphaturia by decreasing renal reabsorption of phosphate. Through this pathway, PTH and FGF23 bring serum [phosphate] back towards physiologically normal levels, and thus act as hormonal regulators of serum [phosphate].

Causes and Consequences of Altered Phosphate Homeostasis

The importance of maintaining serum phosphate within a narrow range is highlighted by the pathologies associated with deviations above or below the normal clinical range. The most common cause of pathologically elevated serum phosphate (hyperphosphatemia) is chronic kidney disease (CKD). Progressive nephron loss leads to inadequate glomerular filtration of phosphate, leading to systemic phosphate buildup. In addition to proposed mechanisms of phosphate toxicity in the cardiovascular system, hyperphosphatemia is independently linked to both cardiovascular-related and all-cause mortality (13). Moreover, hyperphosphatemia has been found to be associated with the development of renal disease (14). Low serum phosphate levels, *i.e.* below the normal range (hypophosphatemia), is often associated with rickets or osteopenia and can be caused by several genetic diseases. X-linked hypophosphatemic rickets (XLHR) is an X-linked dominant disease, and the most common hereditary hypophosphatemia, affecting approximately 1/20,000 individuals (15, 16). XLHR is caused by mutations in the *PHEX* gene. *PHEX* is an enzyme encoded on the X chromosome, that metabolizes osteopontin; a signalling factor that inhibits bone mineralization. In the case of XLHR, mutant *PHEX* fails to metabolize osteopontin adequately, leading to inordinate inhibition of bone mineralization, which is thought to produce, or at least contribute to the clinical phenotype of impaired growth in the lower limbs. FGF23 is also elevated in XLHR contributing further to the hypophosphatemia by inducing renal phosphate wasting, which likely also contributes to the bone phenotype in XLHR. However, the cause of increased FGF23 in XLHR is poorly understood. Two less common forms of hypophosphatemic rickets; autosomal dominant and autosomal recessive hypophosphatemic rickets, both manifest their clinical phenotypes through excessive FGF23 signalling leading to

urinary phosphate wasting (17, 18). A general overview of genetic causes of hypophosphatemia are detailed in *Table 1.1*.

Table 1.1 Genetic causes of hypophosphatemia.

Disease	Mutated protein	Pathophysiology
X-linked hypophosphatemic rickets	PHEX	Impaired bone mineralization, urinary phosphate wasting due to increased FGF23
Autosomal dominant hypophosphatemic rickets	FGF23 (cleavage site)	Urinary phosphate wasting due to impaired FGF23 breakdown
Autosomal recessive hypophosphatemic rickets	Dentin matrix protein 1	Urinary phosphate wasting due to impaired inhibition of FGF23 synthesis
Hereditary hypophosphatemic rickets with hypercalciuria	NaPiIIc	Urinary phosphate wasting due to inadequate phosphate reabsorption from the proximal tubule. Subsequent increase in calcitriol synthesis, leading to excessive calcium absorption causing hypercalciuria

Phosphate Handling in the Developing Mammal

Phosphate balance is defined as the difference between phosphate absorbed by the intestine and phosphate excreted in the urine and feces. During early adolescence in humans, the velocity of bone mineralization is at a lifetime high (19, 20). The high rate of deposition necessitates that developing individuals must establish a sufficiently positive phosphate balance so that adequate mineralization of hydroxyapatite can occur during this critical period. This may generally be accomplished by increased phosphate reabsorption from the renal ultrafiltrate and/or increased phosphate absorption from the small intestine into the systemic circulation.

Intestinal Phosphate Absorption and Renal Phosphate Reabsorption – The Transcellular Pathway

NaPiIIa

NaPiIIa (gene name SLC34A1) is a secondary active transporter whose primary function is the reabsorption of phosphate from the renal ultrafiltrate (*Figure 1.5*). Its predominant site of expression is the proximal tubule, although there is evidence that NaPiIIa may be expressed to some extent in bone and lung (21). In mice, NaPiIIa expression decreases from S1 to S3 of the proximal tubule. However, this appears to only be the case in juxtamedullary nephrons, in contrast to cortical nephrons where NaPiIIa expression is consistent along the length of the proximal tubule (22). The protein is approximately 75 kDa (23). NaPiIIa is an electrogenic transporter; cotransporting 3 Na⁺ for every phosphate ion (24). Higher rates of transport at alkaline versus acidic pH indicate a preference for the divalent form of phosphate (HPO₄²⁻) (25). Homology modeling strongly suggests that NaPiIIa, along with its homologues NaPiIIb and NaPiIIc, are 6 transmembrane domain containing proteins (26). Further evidence supports that

NaPiII transporters assemble into dimers, although each monomer can function independently (27). The affinity for phosphate is approximately 0.3 mM for NaPiIIa at neutral pH (24).

There are approximately 30 known mutations in *SLC34A1* (28–35). Mutations in the NaPiIIa transporter have been identified in children with nephrocalcinosis and hypophosphatemia, as well as renal phosphate losses and poor bone mineralization in adults (29, 30). *SLC34A1* mutations have also been found in infantile idiopathic hypercalcemia (36). It should be noted that most *SLC34A1* mutations have autosomal recessive inheritance with respect to clinical presentation, as a functional allele typically corrects for any abnormalities (37). Consistent with the phenotype observed with mutations in humans, NaPiIIa knockout models in mice produce a phosphate wasting phenotype; suggesting the importance of NaPiIIa in both human and murine phosphate balance (38). Accordingly, pharmacological inhibition of NaPiIIa in mice produces a decrease in serum phosphate (39).

NaPiIIb

NaPiIIb, encoded by *SLC34A2*, is a Na⁺-phosphate cotransporter similar to NaPiIIa in that it has a net charge transfer of +1 and transports Na⁺ and divalent phosphate in a 3:1 ratio (HPO₄²⁻) (25). The major distinction, however, is that NaPiIIb is predominantly expressed in the small intestine and is the main player in apical uptake of phosphate into intestinal enterocytes (40) (*Figure 1.6*). Prior work has demonstrated a role of calcitriol in upregulating NaPiIIb expression; potentially at both the transcriptional and translational/post-translational level depending on the life stage (10, 11). While NaPiIIb is most notably involved in intestinal phosphate transport, it is also expressed in the testes as well as the lungs in type-II pneumocytes

where it is involved in producing surfactant (41). Recent efforts have also revealed that NaPiIIb is expressed in the thick ascending limb of the nephron and may be upregulated in states of renal failure, although the function of NaPiIIb in the thick ascending limb is poorly understood (42). The molecular weight of NaPiIIb varies based on glycosylation status, ranging from approximately 70 to 90 kDa (43, 44). NaPiIIb is a high-affinity transporter, with a reported K_m for Pi of approximately 0.2 mM (45). While the expression profile of NaPiIIb along the small intestine of humans is poorly understood, expression peaks in the ileum in mice and the jejunum in rats (46, 47).

Despite being the primary transporter responsible for transcellular phosphate absorption in the small intestine, there are no known alterations of systemic Pi homeostasis in persons with NaPiIIb mutations. Of note, biallelic mutations in *SLC34A2* have been implicated in pulmonary alveolar microlithiasis, a disease characterized by the deposition of calcium-phosphate microcrystals in the lungs (48). Heterozygous mutations in *SLC34A2* have also been found in patients with testicular microlithiasis (48). In an inducible NaPiIIb knockout mouse model, no change in serum phosphate was observed (40). However, the knockout was associated with a significant decrease in Na^+ -dependent phosphate transport to nearly zero, indicating that NaPiIIb is the principal mediator of transcellular intestinal phosphate absorption. It is plausible that in the absence of NaPiIIb-mediated transport, compensation can occur via paracellular phosphate absorption and renal reabsorption. Despite the lack of a phosphate phenotype associated with *SLC34A2* mutations and knockout models, its importance is highlighted by embryonic death in global knockout models (49).

The pathology associated with hyperphosphatemia in CKD has set the impetus for the investigation of various pharmaceuticals purposed to lower serum phosphate including by inhibition of NaPiIIb-mediated absorption. One such pharmaceutical is ASP3325, which inhibits NaPiIIb with high efficacy (IC₅₀ of 88 nM). Unfortunately, it does not appear to lower serum phosphate in CKD patients (50). Phosphonoformate, also an inhibitor of NaPiIIb, is commonly used to inhibit phosphate transport. However, its nephrotoxicity limits its usage in humans (51).

NaPiIIc

NaPiIIc, encoded by *SLC34A3*, is a 75 kDa protein expressed in the proximal tubule in the kidney (52) (*Figure 1.5*). Along with NaPiIIa, it is responsible for the reabsorption of phosphate from the ultrafiltrate. NaPiIIa has high affinity for phosphate (70 μM) and low expression levels in suckling (pre-weaning) rats, which dramatically increases upon weaning (52). Unlike NaPiIIa and NaPiIIb, NaPiIIc is electroneutral, transporting 2 Na⁺ ions per divalent phosphate ion. While it is principally involved in phosphate reabsorption in the proximal tubule, NaPiIIc may also be expressed to an appreciable extent in the small intestine where it has been proposed to contribute to intestinal phosphate absorption. However, studies in NaPiIIb intestinal specific KO mice argue against this (21). In the proximal tubule, NaPiIIc is expressed almost exclusively in S1 in rats (53).

The importance of NaPiIIc in maintaining phosphate balance is highlighted by the clinical presentation of hereditary hypophosphatemic rickets with hypercalciuria (HHRH). In HHRH patients, mutant NaPiIIc fails to adequately contribute to renal phosphate reabsorption, leading to urinary phosphate loss. Consequently, calcitriol synthesis increases to compensate by

upregulating intestinal phosphate absorption. However, this also contributes increased calcium absorption, which is too much to be completely deposited in bone and therefore produces the hypercalciuric component of HHRH (54). As a result, nephrolithiasis is a common component of the clinical presentation of HHRH. Additionally, phosphate losses due to reduced NaPiIIc expression and/or function are implicated in the short stature and lower extremity deformity commonly observed early in life in HHRH patients (55). The persistence of a clinical phenotype into adulthood suggests the lifetime importance of NaPiIIc in humans (55). An important distinction to draw is that NaPiIIc depletion in mice does not cause phosphate wasting, suggesting that it is more important in human phosphate homeostasis than in mice (56).

Pit1

Encoded by the *SLC20A1* gene, Pit1 is a cotransporter that transports Na⁺ and phosphate with 2:1 stoichiometry. While most notably expressed at the apical membrane of the small intestine, Pit1 is ubiquitously expressed throughout the body. In contrast to the preference of the divalent form of phosphate (HPO₄²⁻) by the transporters encoded by the SLC34 family, Pit1 preferentially transports the monovalent (H₂PO₄⁻) form of phosphate. Similar to the SLC34-encoded transporters, Pit1 is a high-affinity transporter (K_m = 24 μM for phosphate) (57). Pit1, as well as its homologue Pit2, plays a dispensable role in phosphate absorption and may occupy a more noteworthy role in extracellular phosphate sensing via heterodimerization with Pit2 (40, 58).

Ubiquitous tissue distribution of Pit1 suggests its importance in general health, as global Pit1 ablation results in embryonic lethality in mice (59). The phosphate phenotype of an

intestinal-specific Pit1 KO animal has not been documented. However, reduced importance for Pit1 in intestinal phosphate transport can be deduced by the near absence of Na⁺-dependent intestinal phosphate transport in an intestinal-specific NaPiIIIb knockout (40).

Pit2

Pit2 is encoded by *SLC20A2* and, like its homologue Pit1, cotransports Na⁺ and monovalent phosphate (H₂PO₄⁻) in a 2:1 ratio. In addition to its expression in the small intestine, Pit2 has been detected at the messenger RNA level in tissues such as the heart, lung and brain (60). In the kidney, Pit2 is expressed at the apical membrane of epithelial cells in the proximal tubule and thus contributes nominally to phosphate reabsorption (61). Similar to Pit1, Pit2 is a high-affinity phosphate transporter (K_m = 24 μM) and does not play a critical role in phosphate absorption (57, 62).

While Pit2 does not appear to contribute significantly to phosphate absorption under normal conditions, experiments whereby Pit2-null mice were fed a low phosphate diet suggest it may contribute a role under conditions of phosphate scarcity as these animals had elevated circulating calcitriol (62). Since elevated calcitriol is associated with increased intestinal phosphate absorption, this finding is consistent with a non-trivial role of Pit2 in phosphate absorption under low dietary phosphate conditions. Although Pit2 deficiencies have not been linked to diminished phosphate absorption, mutations in Pit2 have been identified as the cause of idiopathic basal ganglia calcification (63).

Pathways of Phosphate Absorption – The Paracellular Pathway

Paracellular flux is the movement of an ion through the tight junction down its electrochemical gradient (*Figure 1.6*). Absorption of phosphate increases linearly with increased luminal phosphate concentration past 1 mM (64, 65). It is highly likely that this linear increase is due to paracellular phosphate flux, as the predominant Na⁺-phosphate transporter NaPiIIb saturates at a low mM luminal phosphate concentration (45). Since aspirated fluid from the human adult jejunum has been reported to range from 0.5 - 17.5 mM, it is likely that paracellular phosphate flux is the predominant mode of dietary phosphate absorption in the adult human (65). A clinical trial involving ASP3325, an inhibitor of NaPiIIb, found that ASP3325 administration did not alter urinary or fecal phosphate excretion in healthy adults, nor did it lower serum phosphate in end stage renal disease patients (50). This suggests that NaPiIIb is not the predominant mode by which phosphate is absorbed, at least in human adults, and that paracellular absorption is sufficient to maintain phosphate balance. Corroborating this, Tenapanor, an NHE3 inhibitor that reduces paracellular permeability to phosphate, was found to reduce serum phosphate in chronic kidney disease patients (66, 67).

Paracellular Phosphate Absorption – The Role of Claudins

The paracellular movement of ions is enabled by a family of proteins called claudins; that are expressed in the tight junction (*Figure 1.7*). In addition to regulating paracellular ion transport, a variety of claudins are up- or down-regulated in certain cancer subtypes and depending on the claudin may be involved in the pathogenesis or amelioration of cancerous states (68–70). There are at least 27 members of the claudin family in humans (71). Claudins have four transmembrane domains and two extracellular loops, the first of which is thought to

confer ion selectivity (72). Claudins can either block or confer paracellular permeability. Generally, of the claudins conferring permeability, they tend to confer paracellular selectivity to either cations or anions of a particular valence. For instance, the interaction between claudin-16 and -19 confers selectivity to the divalent cations calcium (Ca^{2+}) and (Mg^{2+}) (73–75). There are however, claudins for which the role in specific ion selectivity currently isn't known, such as claudin domain-containing protein 1 (cldnd-1), otherwise known as claudin-25 (76).

At present, there is no evidence for paracellular phosphate reabsorption in the kidney; as such, phosphate reabsorption likely occurs almost exclusively via the transcellular pathway. The clinical phenotypes associated with NaPiIIa/c mutations supports the model that the transcellular path is the predominant mode of reabsorption along the nephron, a supposition further supported by the fact that the paracellular pathway is unable to compensate when these genes are mutated (30, 54). Conversely, paracellular phosphate flux is a major player in Pi absorption in the small intestine (77). The identity of the specific claudins that confer phosphate selectivity are not known, although claudin-4 and -23 have been hypothesized to confer paracellular phosphate permeability. Claudin-4 has been shown to select for monovalent anions and against monovalent cations (78). Knopfel et al. found that in rat jejunum, acidic pH conditions, i.e. favouring monovalent phosphate, confer greater paracellular phosphate permeability than alkaline pH conditions, i.e. favouring divalent phosphate (77). Thus, claudin-4 conceivably selects for the monovalent form of phosphate. Claudin-23 has 23.8% sequence homology to claudin-4, and particularly high homology in the first extracellular loop which confers specific ion selectivity. Further, the claudin-23 locus has an upstream vitamin D regulatory site, which was found by examining 5' to the coding region (*Figure 1.8*). Given the role of vitamin D in regulating

phosphate absorption, this is consistent with a potential role of claudin-23 in paracellular phosphate flux.

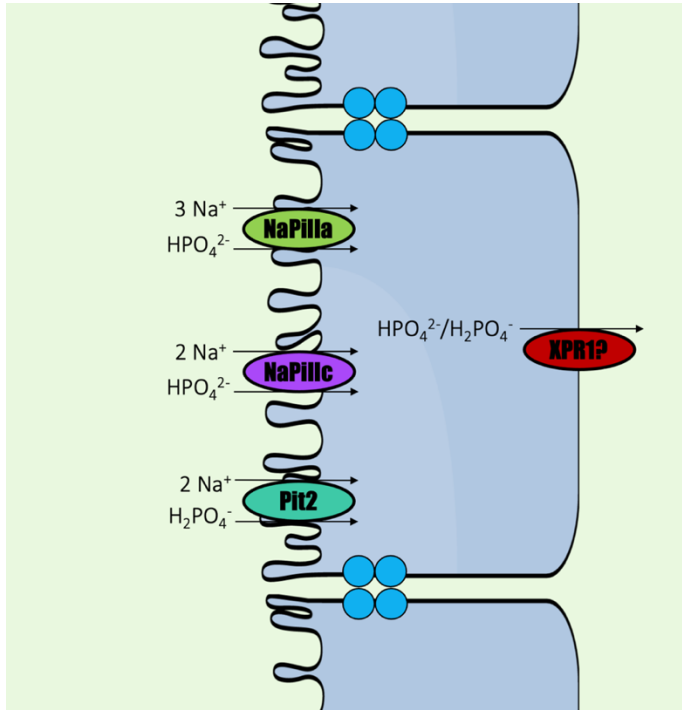


Figure 1.5. Renal phosphate reabsorption in the proximal tubule. NaPiIIa, NaPiIIc and Pit2 are expressed at the apical membrane of the epithelial cell (i.e., facing the tubular lumen) and take up phosphate into the cell via secondary active transport of Na^+ and phosphate. The basolateral mechanism of phosphate extrusion is not known, although XPR1 has been speculated to be responsible, at least in part, for basolateral extrusion of phosphate from the proximal tubule. There is no evidence of paracellular reabsorption of phosphate.

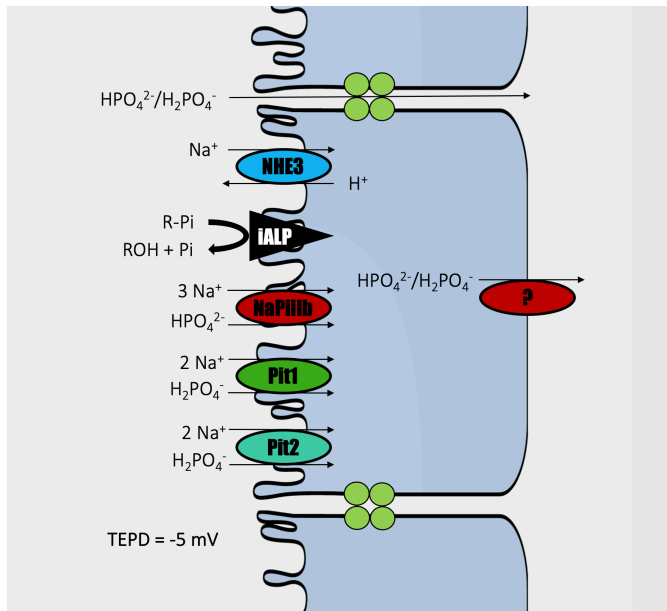


Figure 1.6. Phosphate absorption in the small intestine. In the instance that dietary phosphorus is macromolecule-bound, it must be cleaved from the macromolecule by the hydrolase intestinal alkaline phosphatase prior to absorption, otherwise it will be excreted. The secondary active transporter NaPiIIIb is the principal mediator of apical phosphate uptake into the intestinal enterocyte. Pit1 and Pit2 are secondary active transporters that take up phosphate apically as well, although these transporters have a dispensable role in phosphate homeostasis. The identity of the basolateral phosphate extrusion mechanism is not known. Phosphate may also be absorbed via the paracellular pathway (i.e. through the tight junction); a process indirectly regulated by NHE3.

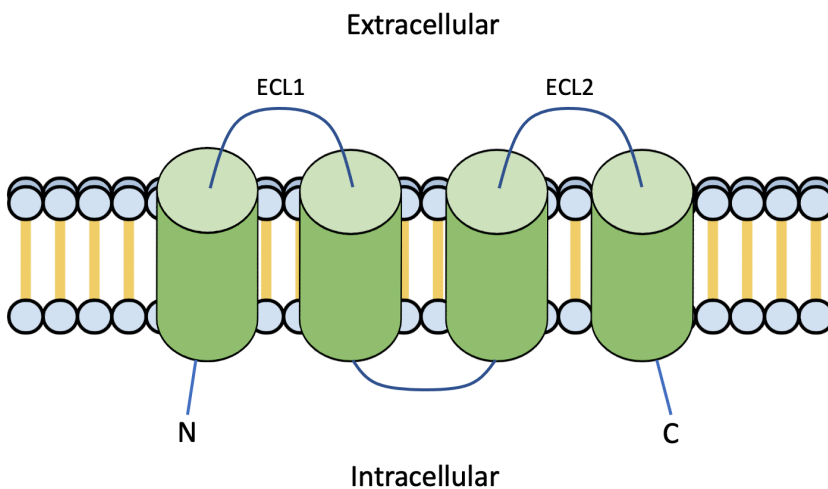


Figure 1.7. General claudin tertiary structure. All claudins possess 4 transmembrane domains, 2 extracellular loops and one intracellular loop. Both N and C termini are cytosolic. Generally, the first extracellular loop; ECL1; dictates the charge/ion selectivity of the specific claudin.

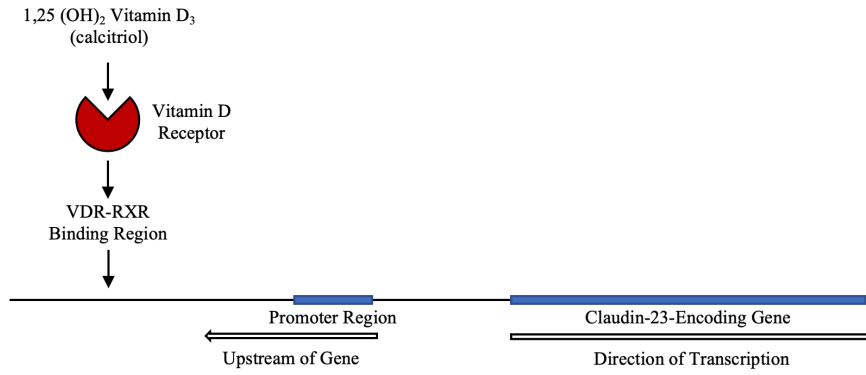


Figure 1.8. The claudin-23 genomic region. Screening upstream of the coding region revealed a vitamin D receptor binding site approximately 5 kilobase pairs upstream, suggesting a potential role of calcitriol in regulating paracellular ion transport.

Intestinal Phosphate Absorption – Alkaline Phosphatase

In the case that a phosphate ion is covalently bound to a macromolecule upon ingestion (organic phosphorus), the phosphate must be cleaved prior to absorption via hydrolytic cleavage from the macromolecule by the intestinal brush border enzyme intestinal alkaline phosphatase (iALP). iALP is a homodimeric hydrolase that is either expressed at the apical membrane of intestinal enterocytes or acts in the intestinal lumen (79). In addition to its role in metabolizing organic phosphorus-containing macromolecules, alkaline phosphatase can be a marker and/or prognostic indicator in disease states such as gastric cancers and osteomalacia (80, 81). The role of iALP in metabolizing nutrients containing phosphate in the small intestine will be discussed presently.

Inorganic phosphate is found in food sources including soda, beer, and many preservative/additive-containing foods. It is thus a very common component of modern diets. What structurally distinguishes inorganic phosphate from organic phosphorus is that it is not bound to any carbon-containing macromolecule upon ingestion, and exists in its free, ionized form. Consequently, inorganic phosphate is more readily absorbed and is thus more bioavailable than organic phosphorus¹. Reported values of the bioavailability of different sources of phosphate are for organic phosphorus ranging from 40-60%, whereas inorganic phosphate bioavailability is often 90-100% (82).

Breast milk is the primary source of dietary phosphate for the nursing infant. While human breast milk [phosphate] values of approximately 4 mM have been reported, it is not

¹ Bioavailability is the percentage of an ingested substance that is absorbed from the gut into systemic circulation.

known the proportion of phosphate in breast milk that is organic versus inorganic (83). It is likely that most of the present organic phosphorus exists in the major proteins found in breast milk, whey and casein.

Developmental Changes in Intestinal Phosphate Homeostasis

Prior to this work, it was clear that neonates have an increased capacity for intestinal phosphate absorption relative to adults, and that this is likely due at least in part to elevated Na⁺-dependent phosphate transport. For instance, Vorland et al. demonstrated via *in situ* jejunal ligation that 10-week-old rats absorb radiolabeled phosphorus at a greater rate than 20- and 30-week-old rats (84). Accordingly, the study showed that NaPiIIb expression was elevated at the message level in the 10-week-old group relative to the older counterparts. Further, a 1992 study was conducted in which small intestinal brush border membrane vesicles (BBMV) were isolated from rabbits aged 2-4, 6, and 12 weeks of age. Across all 3 intestinal segments, BBMV from the 2-4 -week age group displayed greater and more rapid Na⁺-dependent phosphate uptake (85). This study also demonstrated increased iALP activity in the small intestine of the younger rabbits. These results collectively indicate that young mammals have increased absorption of phosphate relative to older animals, and that Na⁺-phosphate cotransport is at least partially responsible for increased phosphate absorption in younger animals. Specifically, NaPiIIb is the likely candidate for this contribution given its primary role in transcellular intestinal phosphate absorption.

Developmental Changes in Renal Phosphate Homeostasis

Akin to increased intestinal phosphate absorption in the neonate, there is also evidence that young mammals maintain a positive phosphate balance by additionally increasing phosphate reabsorption from the renal tubule. In humans, the fractional excretion of phosphate is significantly lower in infants 1-6 months of age compared to adult values; indicative of elevated neonatal reabsorption of phosphate (86). This has also been functionally demonstrated via *in vivo* micropuncture experiments, wherein tubular reabsorption of phosphate was found to be elevated in newborn guinea pigs relative to adults (87). Since renal BBMV from newborn guinea pigs demonstrate a higher V_{max} of Na^+ -dependent phosphate transport than adult counterparts, there likely exists increased activity of NaPiIIa and/or NaPiIIc (88). The work of Segawa et al. however, challenges the paradigm that neonates universally upregulate phosphate reabsorption. This study found that NaPiIIc expression displays a lifetime low in suckling mice, whereupon its abundance increases post-weaning (52). In light of these findings, it is possible that rodents do not increase phosphate reabsorption until a later point in early development. Together however, these findings indicate that elevated tubular phosphate reabsorption is a mechanism by which neonates establish and maintain a positive phosphate balance.

Rationale and Hypothesis

While previous work has shown that developing animals display increased phosphate absorption from the small intestine compared to adults, this work has not been comprehensive with regards to intestinal segment or absorption pathway (transcellular/paracellular). Our present work takes a comprehensive approach to examine both aspects and determine how specifically

young animals upregulate phosphate absorption from the small intestine to contribute to a positive phosphate balance.

We hypothesize that young animals upregulate intestinal phosphate absorption relative to the adult via both a NaPi2b mediated transcellular pathway as well as through the paracellular pathway.

Chapter 2: Materials and Methods

Ethics Approval and Animals

Wild-type FVB/N mice (Taconic Biosciences, Rensselaer, NY) were maintained on a 12-hour light/dark cycle with water and chow (Picolab rodent diet, 8% protein, 0.7% phosphorus). Animal ethics were obtained from the Animal Care and Use Committee, Health Sciences Section (AUP00000213) according to the Guide for the Care and Use of Laboratory Animals (Canadian Council on Animal Care). Pups were weaned from mother's breast milk at 21 days of age.

Isolation of Biological Samples

At the specified age, animals were euthanized via cervical dislocation following induction of the third surgical plane using isoflurane. Concurrently with euthanasia and small bowel mounting for bi-ionic diffusion potential experiments, blood was isolated via puncture of the left ventricle and centrifuged at 10,000 for 5 minutes at 4° C, at which point serum was aliquoted into 1.5 mL Eppendorf tubes, snap frozen on dry ice and stored at -80° C until use. Urine was collected from urine voided onto parafilm at the time of euthanasia, aliquoted into 1.5 mL tubes and snap frozen and stored at -80° C. Small intestine segments were isolated in 1 cm segments. For purposes of tissue isolation, the duodenum, jejunum and ileum were deemed to be 1-4 cm, 10-16 cm, and 22-28 cm distal to the pylorus, respectively. Kidneys were sectioned into quarters. All tissues were transferred into 1.5 mL tubes, snap frozen and stored at -80° C until use.

Real-time Polymerase Chain Reaction

Total RNA was purified from tissue as previously described (89). RNA was purified using Trizol (Invitrogen, Carlsbad, CA) according to the manufactures instructions and then treated with

DNaseI (AmpGrade, Invitrogen, Carlsbad, CA). cDNA was produced from total RNA via reverse transcription of 1 µg of RNA (SensiFAST cDNA Synthesis Kit, Bioline, Cincinnati, OH). Quantification of mRNA of the pertinent genes in wild-type FVB/N mice was performed via TaqMan assay using a QuantStudio 7 Pro 96-well Real-Time PCR System (Thermo Fisher Scientific, Waltham, MA). Primers and probes (Integrated DNA Technologies, San Diego, CA) used for RT-PCR assays are listed in *Table 2.1*. A cycle threshold value of 35 or less was used as the cut-off value for the expression of a given gene at the transcript level, above which it was deemed not expressed. The program used was as follows: 1. Heating from room temperature (25 °C) to 50 °C followed by a holding period of 2 minutes. 2. Heating from 50 °C to 95 °C at a rate of 1.6 °C /second, followed by a 10-minute holding period at 95 °C. 3. 40 cycles of the following: A 15 second holding period at 95 °C followed by cooling at 1.6 °C /second to 60 °C, a 1-minute holding period at 60 °C, followed by heating to 95 °C at 1.6 °C / second. For the housekeeping gene GAPDH, VIC was used as the reporter fluorophore. For all other genes, the reporter fluorophore used was FAM. NFQ-MGB was used as a quencher. Data Analysis was performed using QuantStudio 6 Design & Analysis Software 2.4.3 (Thermo Fisher Scientific, Waltham, MA). Message quantities were normalized to GAPDH.

Table 2.1. Primer and probe sequences for RT-PCR.

Gene	Forward sequence 5' → 3'	Reverse sequence 5' → 3'	Probe sequence 5' → 3'
Cldnd-1	ACATAGCAACTCACGGAGC	TTTACCCTTCGTCAGCTTGG	56-FAM/CCAATCAAC/ZEN/GCCCCAAAGCACAT/3IABkFQ
Claudn-3	CACCAAGATCCTCTATTCTGCG	GGTTCATCGACTGCTGGTAG	56-FAM/CCCCTCAGA/ZEN/CGTAGTCCTTGCG/3IABkFQ
Claudn-4	ID: Mm00515514_s1		
Claudn-7	GATGAGCTGCAAAATGTACGAC	TGGCGACAAACATGGCTAA	56-FAM/CTTAATGG/ZEN/TGGTGTCCCTGGTGT/3IABkFQ
Claudin-23	CCTAGATTGGAGAGGAGTTGG	TGAACTTCTGCCAGTACATCTG	56-FAM/TAGAACCCT/ZEN/GGTCGCCTTCCTCTAA/3IABkFQ
iALP	TCTGCATCTGAGTACCAATTACG	TGATGTACCGTGCCAAGAAAG	56-FAM/TCACCACTC/ZEN/CCACAGACTTCCCT/3IABkFQ
NaPiIIa	ID: Mm00441450_m1		
NaPiIIb	GGAGCACACGAACAAGTAGAG	AGGACACTGGGATCAAATGG	56-FAM/ACCAAAGGG/ZEN/AAGACGCTCTGCAT/3IABkFQ
NaPiIIc	ID: Mm00551746_m1		
Pit1	AATTGGTAAAGCTCGTAAGCCATT	TTCTTGTTCGTGCGTTCATC	56-FAM/CCGTAAGGC/ZEN/AGATCC/3IABkFQ
Pit2	CTCAGGAGGACGCGATCAA	GACCGTGGAAACGCTAATGG	56-FAM/CATGTTGG/ZEN/TTCAGCTG/3IABkFQ
VDR	ID: Mm00437297_m1		
GAPDH	ID: Mm03302249_g1		

Blood and Urine Biochemistry

For the purposes of determining phosphate concentration, serum and urine were diluted 1 in 50 and 1 in 500 in ddH₂O, respectively. Diluted samples were carried through an ion exchange column using 4.5 mM Na₂CO₃ + 1.5 mM NaHCO₃ in ddH₂O as an anion eluent. Standard curves were generated using dilutions of Dionex Combined Five Anion Standard (Thermo Fischer Scientific, Sunnyvale, CA). Data analysis was performed using Chromeleon 6 Chromatography Data System software (Thermo Fisher Scientific).

Ussing Experiments – Tissue Preparation and Mounting

Agarose bridges were made using 200 µL loading tips containing 1.5 % agarose dissolved in 3 M KCl. Prior to mounting, voltage and fluid resistance were set to 0 mM and 0 Ω x cm² respectively, using a VCC 4-channel voltage/current clamp (Physiologic Instruments, San Diego, CA). Zeroing was performed in the presence of 4 mL Krebs Ringers solution (140 mM NaCl, 0.4 mM KH₂PO₄, 2.4 mM K₂HPO₄, 1.2 mM MgCl₂•6H₂O, 1.3 mM calcium

gluconate•1H₂O, 10 mM glucose; pH = 8) in both the apical and basolateral P2400 hemichamber.

Prior to euthanasia, mice were anesthetized using isoflurane. Upon confirmation of the absence of a pain response, euthanasia was performed by cervical dislocation. Removal and linearization of either the duodenum, jejunum or ileum of the small intestine was carried out. This was followed by sectioning and mounting of the tissue on 4 sliders of 0.011 cm² aperture on P2400 chambers with 4 mL of fresh Krebs Ringers solution per hemichamber.

Determination of Paracellular Phosphate Permeability – Bi-ionic Diffusion Potentials

Following tissue mounting, indomethacin was administered bilaterally and tetrodotoxin (TTX) was administered basolaterally for final concentrations of 5 μM and 10 μM, respectively. The dosage at which these compounds were administered was based on previous work from our group (90). Following administration of indomethacin and TTX, recording of voltage readings as a function of time commenced using Acquire and Analyze 2.3 (Physiologic Instruments, San Diego, CA). Tissue was then bathed for 20 minutes. Of note, tissue was bubbled bilaterally and continuously for the duration of the experiment with 95% O₂/5% CO₂. Also of note, the duration of the experiment was carried out under open-circuit conditions. Following the 20-minute initial bathing period, the tissue was pulsed with a 90 μA current a total of three times producing a voltage deflection; the magnitude of which was used to calculate the transepithelial electrochemical resistance (TEER) of the tissue using Ohm's law (voltage = current x resistance). After a 2-minute waiting period, the Krebs Ringers solution in the apical hemichamber was replaced with a low-sodium solution (55 mM NaCl, 0.4 mM KH₂PO₄, 2.4 mM

K_2HPO_4 , 1.2 mM $\text{MgCl}_2 \cdot 6\text{H}_2\text{O}$, 1.3 mM calcium gluconate $\cdot 1\text{H}_2\text{O}$, 10 mM glucose, 175 mM mannitol; pH = 8). The magnitude of the voltage deflection was then taken 2.5 minutes following replacement with the low-sodium solution. The apical solution was then replaced with fresh Krebs Ringers solution, followed by a 5-minute waiting period. The tissue was then pulsed again 3 times at 90 μA , followed by a 2-minute waiting period. The apical Krebs Ringers solution was then replaced with a high phosphate-containing solution (140 mM NaH_2PO_4 , 0.4 mM KH_2PO_4 , 2.4 mM K_2HPO_4 , 1.2 mM $\text{MgCl}_2 \cdot 6\text{H}_2\text{O}$, 1.3 mM calcium gluconate $\cdot 1\text{H}_2\text{O}$, 10 mM glucose; pH = 8). Of note, calcium gluconate was added to the high phosphate solution immediately prior to the experiment. Following a 2.5-minute waiting period after administration of the high-phosphate solution, the magnitude of the voltage deflection was recorded. The apical solution was then replaced with fresh Krebs Ringers solution. A 5-minute waiting period followed, upon which the tissue was pulsed again with a 90 μA current. Following a 2-minute waiting period, forskolin was administered bilaterally at a final concentration of 10 μM . The voltage response was recorded 3 minutes after the administration of forskolin.

Using the magnitude of voltage deflections in response to the low-sodium and high-phosphate solutions, the paracellular permeability to sodium normalized to chloride ($P_{\text{Na}}/P_{\text{Cl}}$) and paracellular permeability to phosphate (P_{Pi}) were calculated using *equation 1*, *equation 2*. The absolute paracellular permeability to sodium (P_{Na}) and chloride (P_{Cl}) were calculated using the Kimizuka-Koketsu equation (91).

A supplementary chart displaying the ionic composition of each buffer used in the dilution potentials is available (*Table 2.2*). Additionally, a supplementary figure outlining the bi-ionic diffusion potential protocol is depicted in *Figure 2.1*.

$$E_m = \frac{RT}{F} \ln \left(\frac{P_{Na}[Na]_{bl} + P_{Cl}[Cl]_{ap}}{P_{Na}[Na]_{ap} + P_{Cl}[Cl]_{bl}} \right)$$

Equation 1. Goldman-Hodgkin-Katz Equation for paracellular permeability with respect to sodium and chloride; the predominant species in the low-sodium buffer. E_m = Membrane potential; R = Gas constant; $8.314 \text{ J}\cdot\text{mol}^{-1}\cdot\text{K}^{-1}$; T = Temperature in Kelvins; F = Faraday's constant; $96,485 \text{ J}\cdot\text{K}^{-1}\cdot\text{mol}^{-1}$; P_{Na} = Paracellular permeability to sodium; P_{Cl} = Paracellular permeability to chloride; ap = Apical; bl = basolateral; P = Permeability with respect to the given ion.

$$P_{Pi^{2-}} = \left(\frac{P_{Na}(1 + e^u)([Na]_{bl} - [Na]_{ap}e^u) + P_{Cl}(1 + e^u)([Cl]_{ap} - [Cl]_{ap}e^u)}{4([Pi^{2-}]_{bl}e^{2u} - [Pi^{2-}]_{ap})} \right)$$

Equation 2. Goldman-Hodgkin-Katz equation for divalent phosphate (HPO_4^{2-}); derived from the Goldman-Hodgkin-Katz flux equation. ap = Apical; bl = basolateral; P = Permeability with respect to the given ion; $u = V_m F / RT$ (for simplicity of depiction above); where V_m = Membrane potential; R = Gas constant; T = Temperature.

Determination of Net Transcellular Phosphate Flux

Following tissue preparation and mounting, indomethacin and TTX were administered as described in the previous section. As with the bi-ionic diffusion potential experiments, tissue was bathed for 20 minutes under open-circuit conditions post-mounting, followed by pulsing with a $90 \mu\text{A}$ current. Following a 2-minute waiting period under an open circuit, the voltage was clamped to 2 mV and 3 additional pulses were administered to the tissue at $90 \mu\text{A}$. Voltage was then clamped to 0 mV to eliminate the driving force for paracellular phosphate flux. At this time, $3 \mu\text{Ci}$ of the radioisotope phosphorus 33 (P-33) (American Radiolabeled Chemicals, St. Louis, MO) were administered to either the apical or basolateral hemichamber corresponding to each channel. In each chamber, the hemichamber in which P-33 was administered is referred to as the “hot” side, where the hemichamber not receiving P-33 is referred to as the “cold” side. Upon

administration of P-33, 50 μ L samples of Krebs Ringers solution were taken and collected from the “hot” and “cold” side of each chamber in duplicate and quadruplicate, respectively. Samples were collected in this fashion in 15-minute time increments at $t = 0$ minutes (immediately following P-33 administration), $t = 15$ minutes, $t = 30$ minutes, $t = 45$ minutes, and $t = 60$ minutes. Samples were collected in 7 mL polyethylene scintillation vials (Fischer Scientific), containing 4 mL scintillation fluid (PerkinElmer, Solon, OH). Following the 5 collection periods, all 4 channels were restored to open-circuit conditions. Recording of voltage readings was followed by pulsing at 90 μ A. As with the bi-ionic dilution potential experiments, two minutes after pulsing, forskolin was administered bilaterally for a final concentration of 10 μ M. After a 3-minute waiting period, the change in voltage pre- and post-forskolin administration was recorded, followed by a second series of pulses at 90 μ A.

Counts per minute (CPM) in each scintillation vial were determined using an LS 6000 Liquid Scintillation Counter (Beckman Coulter). The apical-to-basolateral and basolateral-to-apical movement of P-33 determined by the change in CPM was converted to the moles of phosphate in the Krebs Ringers solution crossing the epithelium in each respective direction. In this way, both the apical \rightarrow basolateral and basolateral \rightarrow apical phosphate flux was determined. Phosphate flux was calculated by taking the rate of P-33 appearance in the cold hemichamber (i.e. the hemichamber not spiked with P-33) divided by the specific activity of P-33 in the hot hemichamber. Finally, this was normalized to 0.011 cm^2 ; the surface area of the aperture. The net phosphate flux was then determined using the following formula:

$$\text{Net flux} = (\text{apical} \rightarrow \text{basolateral flux}) - (\text{basolateral} \rightarrow \text{apical flux})$$

Inhibition of NaPiIIb in Juvenile Apical to Basolateral Flux

NTX1942, a specific inhibitor of NaPiIIb, was acquired from Ardelyx (92). The experimental setup was identical to net transcellular flux studies with the following notable exceptions: 1. Mice used were solely juvenile mice; P7-14 days of age. 2. The only studied segments were the jejunum and ileum of the small intestine, which had significantly increased transcellular fluxes measured at this age relative to older animals. 3. In all 4 channels, the only “hot” sides, that is, spiked with P-33, were the apical hemichambers i.e. we only measured apical to basolateral fluxes.

The solution containing NTX1942 comprised Krebs Ringers solution and 50 μM NTX1942 (herein referred to as Krebs + NTX1942), approximately 10 times the compound's IC50 with respect to NaPiIIb. To produce a solution with a final [NTX1942] of 50 μM , a 1 mM NTX1942 stock solution was made using ddH₂O as solvent. The NTX1942 stock solution was added to Krebs Ringers solution at 0.5% by volume for a final concentration of 50 μM NTX1942. To make Krebs Ringers + vehicle solution (herein referred to as Krebs + vehicle), ddH₂O was added to Krebs Ringers solution at 0.5% by volume.

Following tissue preparation and mounting, 4 mL Krebs + NTX1942 were added to each apical hemichamber of channels 1 and 2. To achieve equal solution osmolarity in either hemichamber, 4 mL Krebs + vehicle was administered in the basolateral hemichambers of channels 1 and 2. In the remaining channels 3 and 4, 4 mL Krebs + vehicle was administered in each hemichamber.

Following this, the experimental design was identical to that which was used to determine net transcellular phosphate flux.

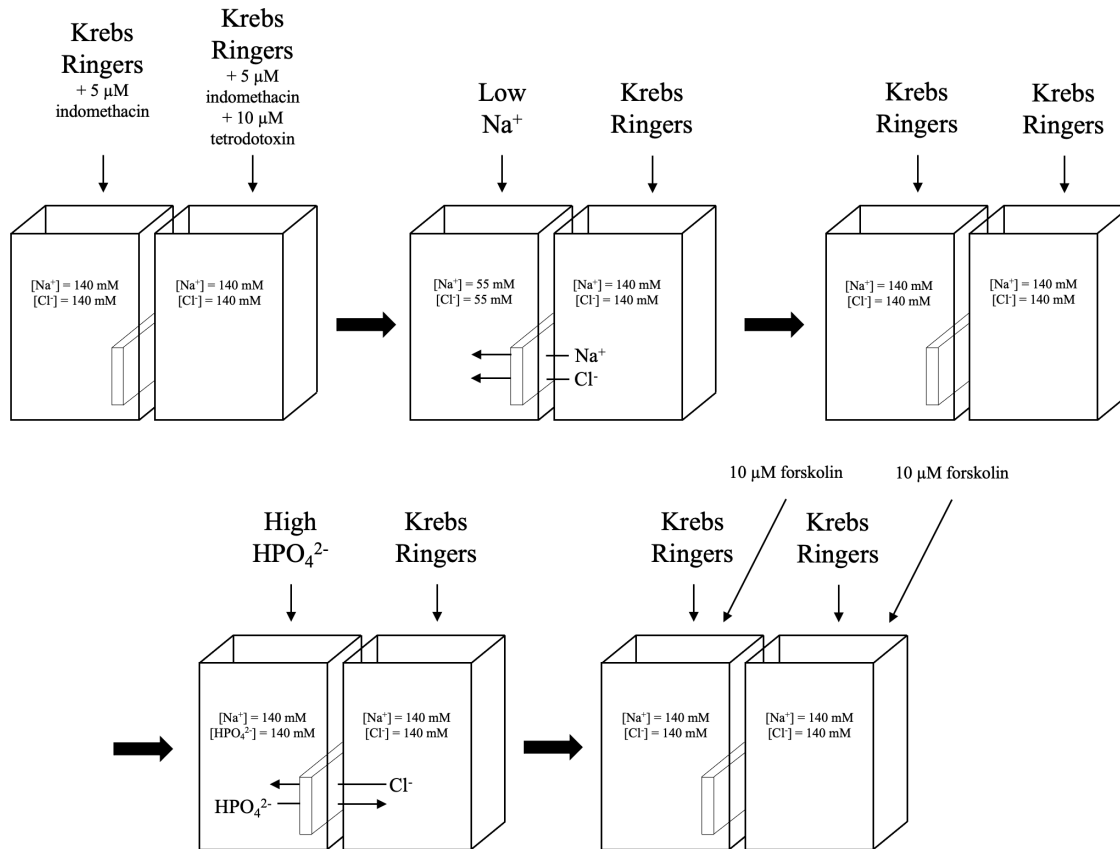


Figure 2.1 Bi-ionic diffusion potential protocol. Arrows displaying transepithelial ion flux indicate the gradient-driven flux of the respective ions.

Statistical Analysis

All statistical analysis and figure design was performed in Prism 8 GraphPad. Data in all figures are presented as the mean \pm standard deviation. Normality of distribution was determined using the Shapiro-Wilk test ($\alpha > 0.05$). Statistical differences between groups for all RT-PCR data were determined using one-way ANOVA ($p < 0.05$). With respect to data acquired in bi-ionic diffusion potential and P-33 flux experiments, statistical differences between the juvenile and adult age groups were determined using unpaired t-tests ($p < 0.05$). Outliers were removed from data sets using the ROUT method ($Q = 1\%$).

Table 2.2. Ionic composition of buffers used in bi-ionic diffusion potential experiments.

	Buffer Component							
	NaCl (mM)	NaH ₂ PO ₄ (mM)	KH ₂ PO ₄ (mM)	K ₂ HPO ₄ (mM)	MgCl ₂ •6H ₂ O (mM)	Calcium gluconate•1H ₂ O (mM)	Glucose (mM)	Mannitol (mM)
Krebs Ringer's	140		0.4	2.4	1.2	1.3	10	
Low sodium	55		0.4	2.4	1.2	1.3	10	175
High phosphate		140	0.4	2.4	1.2	1.3	10	

Chapter 3: Results

Blood and Urine Phosphate Levels at Different Ages

Consistent with prior literature, the serum phosphate concentration was significantly higher in P7-14 mice when compared to adults (3, 4). Further, urine phosphate normalized to creatinine in the younger age group was also greater than adult values (*Figure 3.1*).

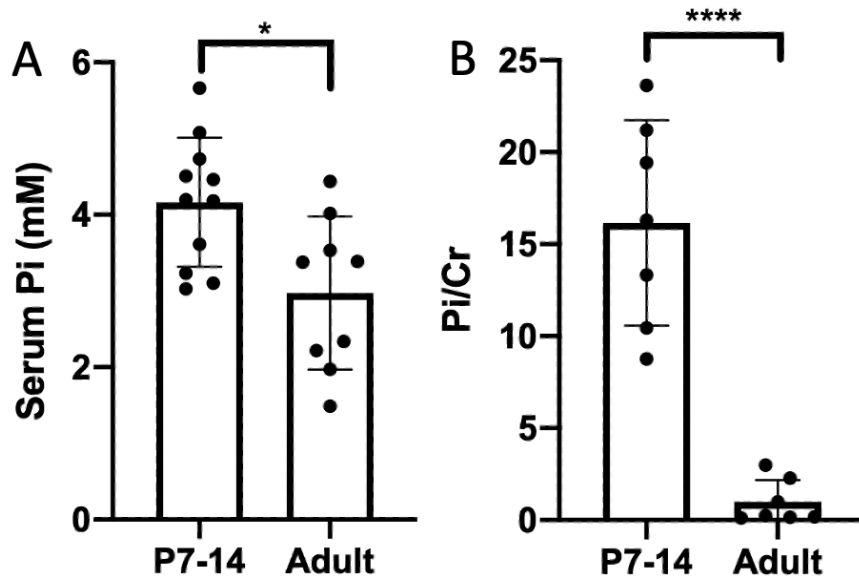


Figure 3.1. Serum and urine biochemistry in juvenile and adult mice. A) Serum phosphate concentration and B) Urine phosphate normalized to creatinine in juvenile (P7-14-day-old) and adult (8-17-weeks-old) mice. Statistical significance assessed using 2-tailed t test ($P < 0.05$).

Changes in Gene Expression of the Transcellular Pathway at Different Developmental Ages in the Kidney

The developmental expression of both major secondary active Na⁺-phosphate cotransporters in the proximal tubule follows a similar profile. The renal expression of both NaPiIIa and NaPiIIc-encoding transcripts are expressed at low levels from P1-7 days. However, this is followed by a significant increase in expression at P14 which is sustained until 6 months for NaPiIIa. NaPiIIc expression however decreases by 2 months to levels similar to P7, which are still greater than P1 (*Figure 3.2*). Expression of Pit1 and Pit2 is greatest at P1 and gradually decreases to roughly 50% by 6 months of age.

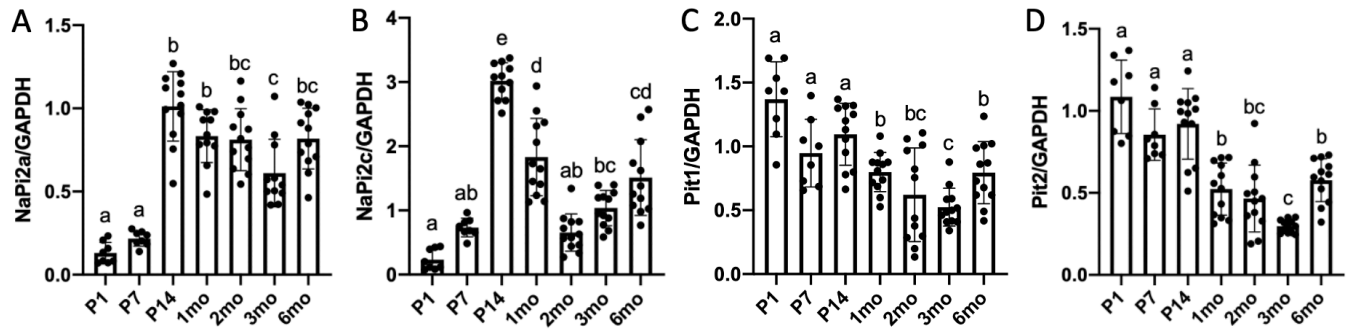


Figure 3.2 Developmental changes in transporters involved in transcellular renal phosphate reabsorption. Shown are transcript abundance levels across development, normalized to GAPDH, of A) NaPiIIa, B) NaPiIIc, C) Pit1 and D) Pit2. Statistical significance assessed using one-way ANOVA ($P < 0.05$).

Despite Significantly Increased NaPiIIb Expression at P7 and P14 in the Duodenum, there is Not Increased Net Phosphate Flux

In the duodenum of the small intestine, NaPiIIb expression peaked at P7 days, then declined significantly at P14 days. At one month of age and onwards, no NaPiIIb transcript was detected in the duodenum. Pit1, one of the two Na⁺-phosphate transporters with a relatively dispensable role in phosphate absorption (40), displayed no discernible peak in the duodenum. Pit2 however displayed a clear peak between P1 and P14, whereupon transcript abundance decreased to post-weaning levels similar to adult values. With respect to iALP expression in the duodenum, message abundance increased gradually up to 1 month of age and persisted at this level of abundance to 6 months. Interestingly, mRNA levels encoding the VDR in the duodenum were increased dramatically post-weaning and remained elevated to 6 months of age (*Figure 3.3*). Despite significantly increase NaPiIIb in the duodenum there was no difference in unidirectional nor net transcellular phosphate flux across this segment between P7-P14 mice and 2-month-old animals (*Figure 3.3 F-H*).

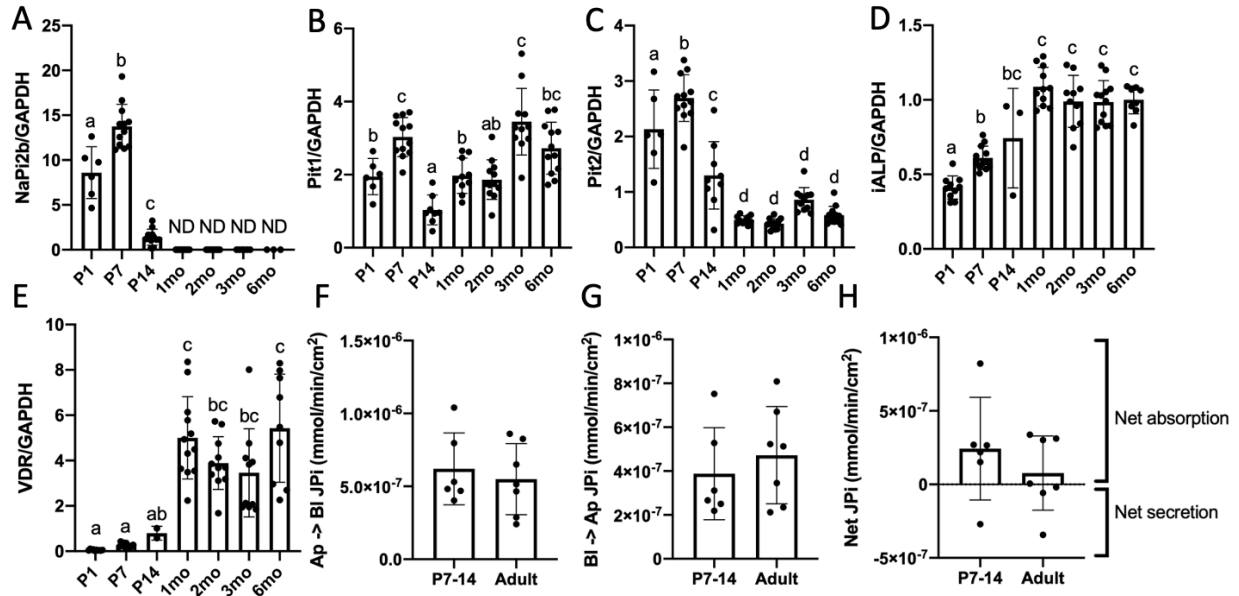


Figure 3.3 Expression and function of the transcellular phosphate transport pathway in the duodenum. mRNA transcript abundance across development of A) NaPiIIb, B) Pit1 C) Pit2 D) Intestinal alkaline phosphatase (iALP), and E) Vitamin D receptor. All transcript quantity values were normalized to quantity of GAPDH. Presented in F) and G) are, apical-to-basolateral, and basolateral-to-apical phosphate flux in juvenile (P7-14-day-old) versus adult mice respectively. The difference between apical-to basolateral and basolateral-to-apical flux was used to calculate H) Net phosphate flux. Statistical significance between groups in gene expression and flux data determined using, respectively, one-way ANOVA and 2-tailed t test ($P < 0.05$).

Significantly Increased NaPiIIb Expression Before P14 in the Jejunum Confers Increased Net Phosphate Flux

Similar to the expression profile of NaPiIIb in the duodenum, messenger RNA levels in the jejunum displayed peak values at P1-P7 days of age followed by a precipitous decrease between P7 and P14 days, and nondetectable levels from 1-6 months of age. Also akin to the findings observed in the duodenum, Pit1 displayed no clear developmental trend and Pit2 expression peaked between P1 and P14, followed by a post-weaning decrease to adult values. Similarly, iALP expression peaked between P1 and P7 days of age, and declined to adult values by P14. VDR transcript abundance in the jejunum was found to increase steadily across development from P1– 6 months (*Figure 3.4*).

In order to assess whether increased NaPiIIb expression at P7-14 conferred increased net transcellular phosphate flux across this segment we performed unidirectional phosphate flux studies at this age and in older; 2-4-month-old mice, in Ussing chambers. We then calculated the difference in flux in order to determine net flux at the two ages. In contrast to the duodenum, net phosphate flux was increased in the younger animals relative to the adults. Surprisingly this was due to reduced basolateral to apical flux in the younger mice. We postulated this may be due to recycling of basolateral phosphate in the apical chamber through a transcellular pathway via NaPiIIb. To assess if there was increased NaPiIIb activity in the young mice we measured apical to basolateral phosphate flux across this segment in the young mice in the presence and absence of the NaPiIIb inhibitor NTX1942. This significantly decreased apical to basolateral phosphate flux, consistent with increased NaPiIIb mediated net flux across the jejunum in the younger animals.

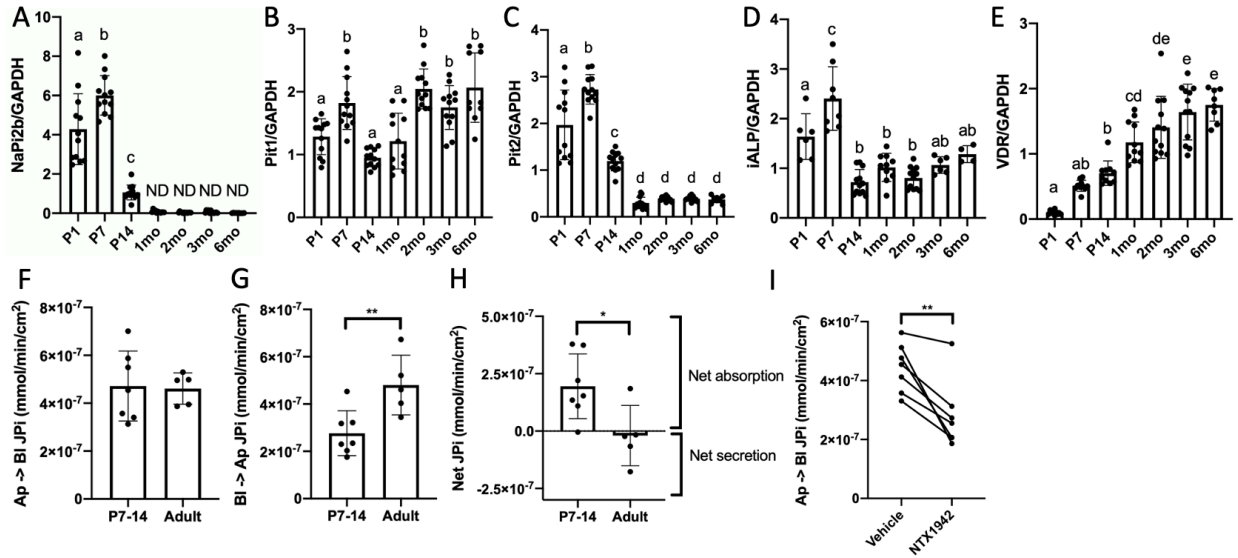


Figure 3.4. Expression and function of the transcellular phosphate transport pathway in the jejunum. Phosphate transport transcript abundance across development of A) NaPiIb, B) Pit1 C) Pit2, D) Intestinal alkaline phosphatase (iALP), and E) Vitamin D receptor. Transcript quantities were normalized to GAPDH. Presented in F) and G) are apical-to-basolateral and basolateral-to-apical phosphate flux, respectively, in juvenile (P7-14-day-old) versus adult mice. The difference between these two flux values in each experiment was used to calculate H) Net phosphate flux. Shown in I) is the effect of the NaPiIb inhibitor NTX1942 on apical-to-basolateral transcellular phosphate flux in juvenile (P7-P14) mice. Statistical differences between groups in gene expression and flux data assessed using one-way ANOVA and 2-tailed t test, respectively ($P < 0.05$).

Significantly Increased NaPiIIb Expression at P14 in the Ileum Confers Increased Net Phosphate Flux

In the ileum, NaPiIIb transcript levels peaked prior to weaning, similarly to that which was observed in the duodenum and jejunum. However, unlike the proximal segments, NaPiIIb expression persisted into adulthood in the ileum. As with the previous two small bowel segments, Pit1 transcript abundance followed no discernible trend and Pit2 expression peaked pre-weaning followed by a decline to adult levels post-weaning. While iALP did not exhibit a clear developmental trend, the highest expression at the message level was observed at P14. Similar to the developmental trend in the duodenum, VDR transcript levels in the ileum display low levels prior to weaning, followed by a dramatic increase at 1 month to adult levels (*Figure 3.5*).

In order to assess whether increased NaPiIIb expression at P7-14 conferred increased net transcellular phosphate flux across this segment we performed unidirectional phosphate flux studies at this age and in older, 2-4-month-old mice, in Ussing chambers as we did for the other segments. We then calculated the difference in flux in order to determine net flux at the two ages. Consistent with the results from the jejunum net phosphate flux was increased in the younger animals relative to the adults in the ileum. This was also due to reduced basolateral to apical flux in the younger mice as per the jejunum. Again, we hypothesize that this is due to increased recycling of basolateral phosphate in the apical chamber through a transcellular pathway mediated by NaPiIIb. To assess if there was increased NaPiIIb activity in the young mice we measured apical to basolateral phosphate flux across the ileum in the young mice in the presence and absence of the NaPiIIb inhibitor NTX1942. This revealed significantly decreased flux, consistent with increased NaPiIIb mediated net flux across the ileum in the younger animals.

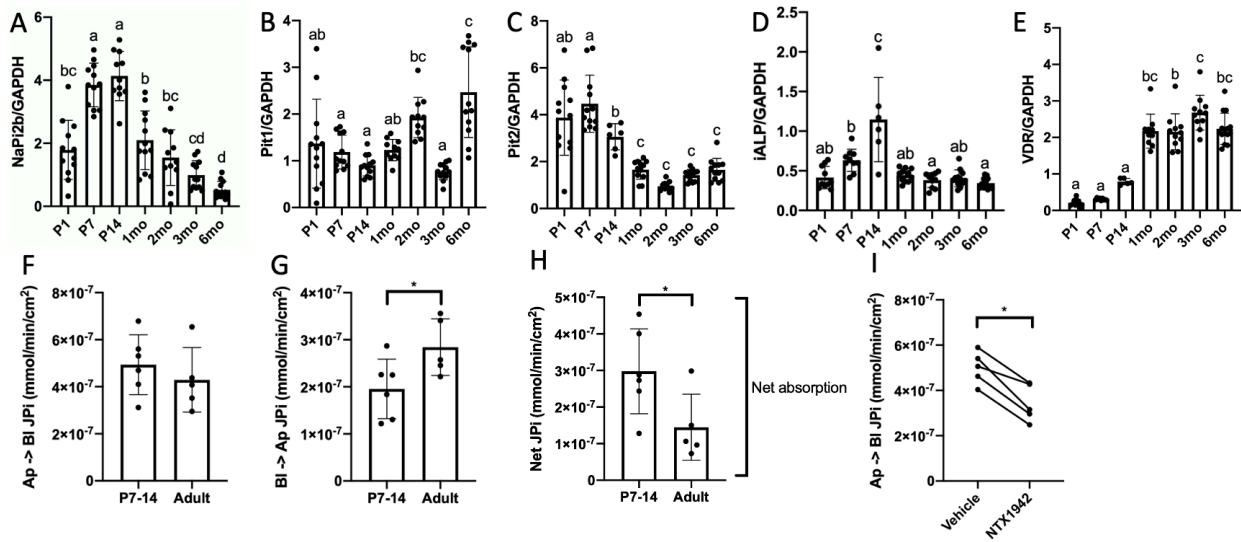


Figure 3.5. Expression and function of the transcellular phosphate transport pathway in the ileum. The transcript abundance of transcellular phosphate transporters, normalized to GAPDH, A) NaPiIIb, B) Pit1, C) Pit2, D) Intestinal alkaline phosphatase (iALP), and E) Vitamin D receptor. Shown in F) and G) are apical-to-basolateral and basolateral-to-apical phosphate flux, respectively, in juvenile (P7-14-day-old) versus adult mice. These values were used to calculate H) Net phosphate flux. Presented in I) is the effect of the NaPiIIb inhibitor NTX1942 on apical-to-basolateral phosphate flux in young mice. Statistics with respect to gene expression and flux data assessed using one-way ANOVA and 2-tailed t test, respectively ($P < 0.05$).

Paracellular Pathway Gene Expression and Permeability across Development in the Duodenum

The expression of claudin domain-containing protein 1 (cldnd-1; also known as Cldn-25) in the duodenum showed a modest but general upward trend across the studied developmental period. Cldn-3, a claudin responsible in part for sealing the tight junction, did not display a distinct trend in expressional changes between P1 and 6 months. A clear peak in Cldn-4 messenger RNA levels however was observed at 7 days of age in the duodenum. The Na⁺-conducting Cldn-7 also displayed a clear peak at P7 in the duodenum. Unlike Cldn-4, Cldn-23; the second claudin hypothesized to be involved in paracellular phosphate absorption, did not have a distinct developmental trend in the duodenum (*Figure 3.6*).

In order to examine functional changes in the paracellular phosphate transport pathway we measured paracellular phosphate permeability. This was accomplished by mounting intestinal segments in Ussing chambers, then sequentially measuring TEER and relative sodium to chloride ratio via generating a dilution potential. Finally, we measured relative phosphate to chloride permeability by measuring a bionic phosphate to chloride diffusion potential by placing asymmetric phosphate and chloride containing solutions on either side of the hemi chambers. We observed no difference in TEER P_{Na}/P_{Cl} or P_{Na} at the different ages. We did however find reduced P_{Cl} , P_{Pi}/P_{Cl} and P_{Pi} in the older mice, consistent with increased phosphate permeability across the duodenum in the younger mice.

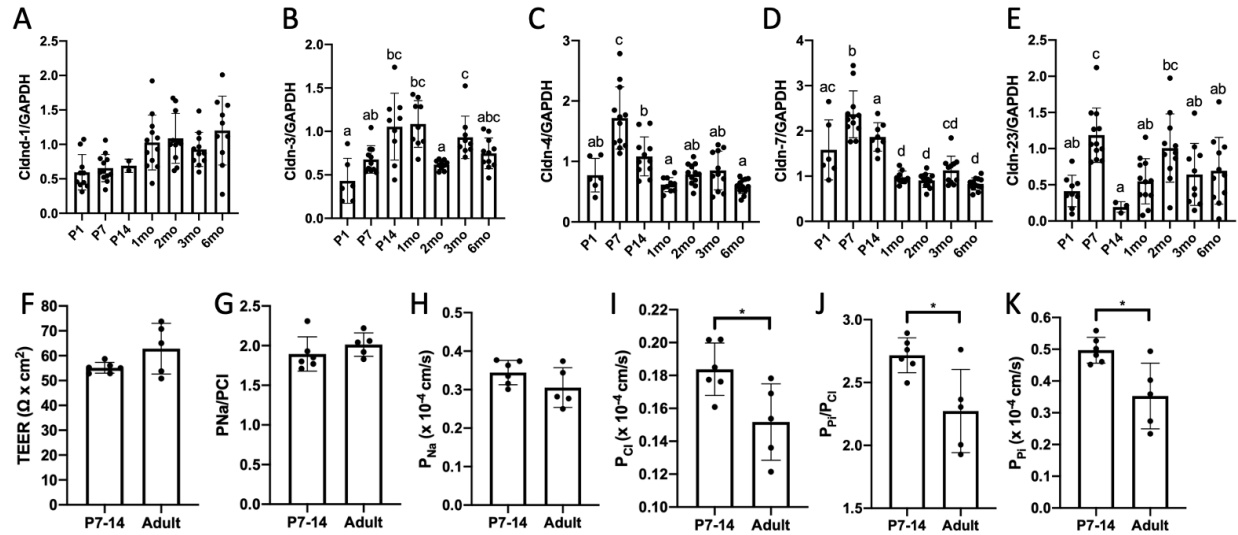


Figure 3.6 Gene expression profile and functional differences in paracellular phosphate permeability across development in the duodenum. Transcript abundance, normalized to GAPDH, of A) Cldnd-1, B) Claudin-3, C) Claudin-4 D) Claudin-7 and E) Claudin-23 across developmental ages. Ussing chamber studies were performed *ex vivo* on the duodenum from juvenile and adult duodenum used to determine F) Transepithelial electrochemical resistance (TEER), G) Paracellular sodium permeability normalized to chloride permeability, H-I) Un-normalized paracellular sodium and chloride permeability, respectively, J) Paracellular phosphate permeability normalized to chloride permeability, and K) Absolute paracellular permeability to phosphate. Statistics with respect to gene expression and *ex vivo* electrophysiology data assessed using one-way ANOVA and 2-tailed t test, respectively ($P < 0.05$).

Paracellular Pathway Gene Expression and Permeability across Development in the Jejunum

In contrast to the expression profile in the duodenum, *cldnd-1* transcript abundance in the jejunum remained remarkably consistent across development. Also in contrast to the findings in the proximal-most segment of the small bowel, *cldn-3* expression clearly trended upwards between P1 and 6 months. Similar to the duodenum, however, was the distinct developmental peak in both *Cldn-4* and *-7* messenger RNA levels at 7 days of age. Contrasting the lack of a developmental profile in the duodenum, *Cldn-23* mRNA abundance displayed a clear peak at P7 similar to that observed with respect to *Cldn-4* and *-7* in the Duodenum (*Figure 3.7*).

We also performed Ussing chamber permeability studies on jejunal segments isolated *ex vivo*. In the jejunum we observed decreased TEER in the young mice, but not altered P_{Na}/P_{Cl} . We did however find increased P_{Na} , P_{Cl} and P_{Pi} relative to adults. Again, we observed increased P_{Pi}/P_{Cl} consistent with both increased paracellular phosphate permeability across the jejunum of younger mice, which is even greater than increase in chloride permeability at this age.

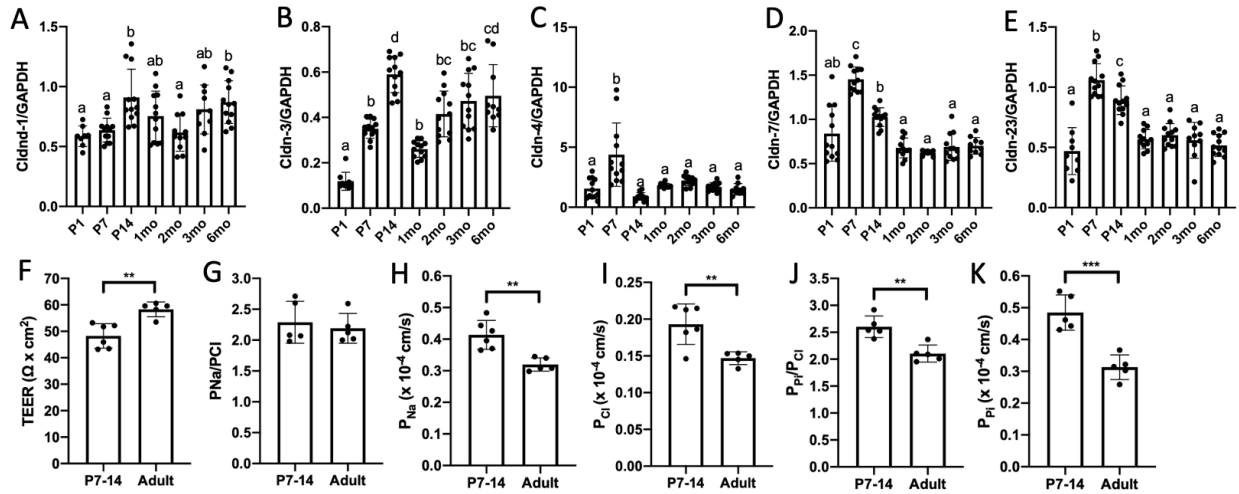


Figure 3.7 Gene expression profile and functional differences in paracellular phosphate permeability across development in the jejunum. Transcript abundance, normalized to GAPDH, of A) Cldnd-1, B) Claudin-3, C) Claudin-4 D) Claudin-7 and E) Claudin-23 across developmental ages. Ussing chamber studies were performed *ex vivo* on the duodenum from juvenile and adult duodenum used to determine F) Transepithelial electrochemical resistance (TEER), G) Paracellular sodium permeability normalized to chloride permeability, H-I) Un-normalized paracellular sodium and chloride permeability, respectively, J) Paracellular phosphate permeability normalized to chloride permeability, and K) Absolute paracellular permeability to phosphate. Statistics with respect to gene expression and *ex vivo* electrophysiology data assessed using one-way ANOVA and 2-tailed t test, respectively ($P < 0.05$).

Paracellular Pathway Gene Expression and Permeability across Development in the Ileum

Comparable to the trend in the jejunum, *cldn-3* message abundance exhibited a distinct upward trend across the analyzed period from 1 day to 6 months of age. While *cldn-4* transcript levels displayed a clear peak at P7 in the duodenum and jejunum of the small intestine, no distinguishable trend could be observed in the ileum with respect to *cldn-4*. Opposite to the general downward trend in *cldn-7* mRNA values across development in the two proximal segments, *cldn-7* message levels trended upwards in the ileum. As with the jejunum, *cldn-23* abundance showed a distinct developmental peak at 7-14 days of age (*Figure 3.8*).

We also performed Ussing chambers permeability studies on ileal segments isolated *ex vivo*. As in the jejunum we observed decreased TEER in the young mice, but not altered P_{Na}/P_{Cl} . As with the jejunum however, we did find increased P_{Na} , P_{Cl} and P_{Pi} in juvenile mice. Again, we observed increased P_{Pi}/P_{Cl} consistent with increased paracellular phosphate permeability across the ileum of younger mice, which is greater than the increase in chloride permeability in the young age group.

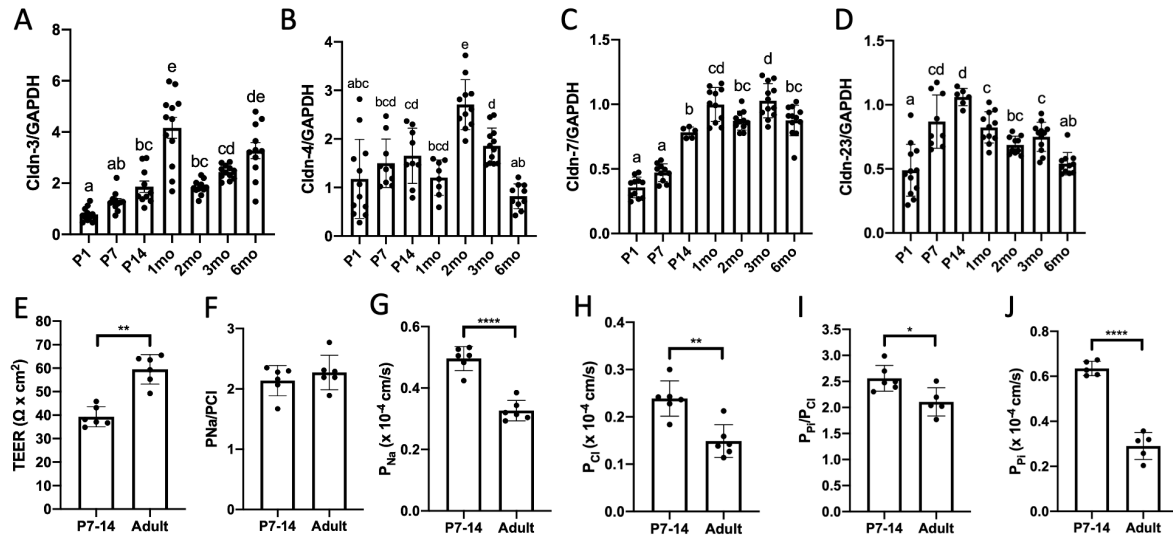


Figure 3.8. Gene expression profile and functional differences in paracellular phosphate permeability across development in the ileum. Transcript abundance, normalized to GAPDH, of A) Cldnd-1, B) Claudin-3, C) Claudin-4 D) Claudin-7 and E) Claudin-23 across developmental ages. Ussing chamber studies were performed *ex vivo* on the duodenum from juvenile and adult duodenum used to determine F) Transepithelial electrochemical resistance (TEER), G) Paracellular sodium permeability normalized to chloride permeability, H-I) Un-normalized paracellular sodium and chloride permeability, respectively, J) Paracellular phosphate permeability normalized to chloride permeability, and K) Absolute paracellular permeability to phosphate. Statistics with respect to gene expression and *ex vivo* electrophysiology data assessed using one-way ANOVA and 2-tailed t test, respectively ($P < 0.05$).

Given the apparent primacy of NaPiIIb in mediating transcellular phosphate absorption across the small bowel we compared the relative expression of NaPiIIb across all segments at all ages. NaPiIIb mRNA expression was greatest at P7 in the duodenum, however it is clear that NaPiIIb expression is lost from the duodenum and jejunum by 1 month. It is also clear that while there is more NaPiIIb in the ileum at younger ages, it is less than the more proximal segments. However, ileal NaPiIIb expression is retained throughout all adult ages (*Figure 3.9*). Comparison of the other genes examined across all ages and small intestine segments is provided in *Figures 3.10 - 3.17*.

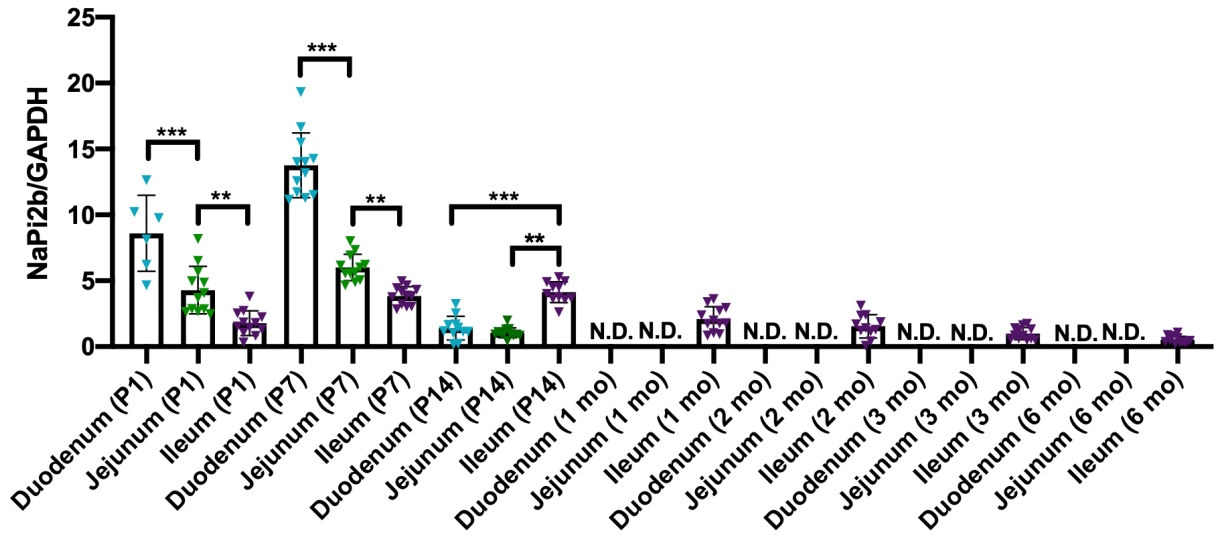


Figure 3.9. NaPiIib expression in all assessed ages and small bowel segments. All NaPiIib message levels normalized to the housekeeping gene GAPDH. Statistical differences between segments at each given age assessed using one-way ANOVA ($P < 0.05$).

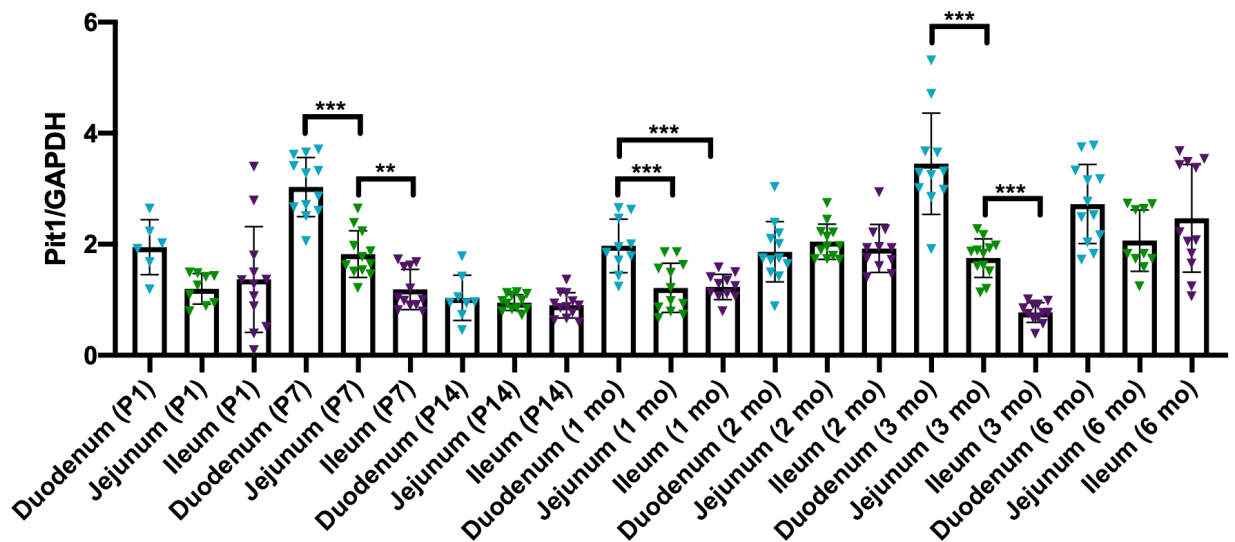


Figure 3.10. Pit1 expression in all ages and all small bowel segments. All messenger RNA levels were normalized to GAPDH. Statistical differences between segments at each respective age determined using one-way ANOVA ($P < 0.05$).

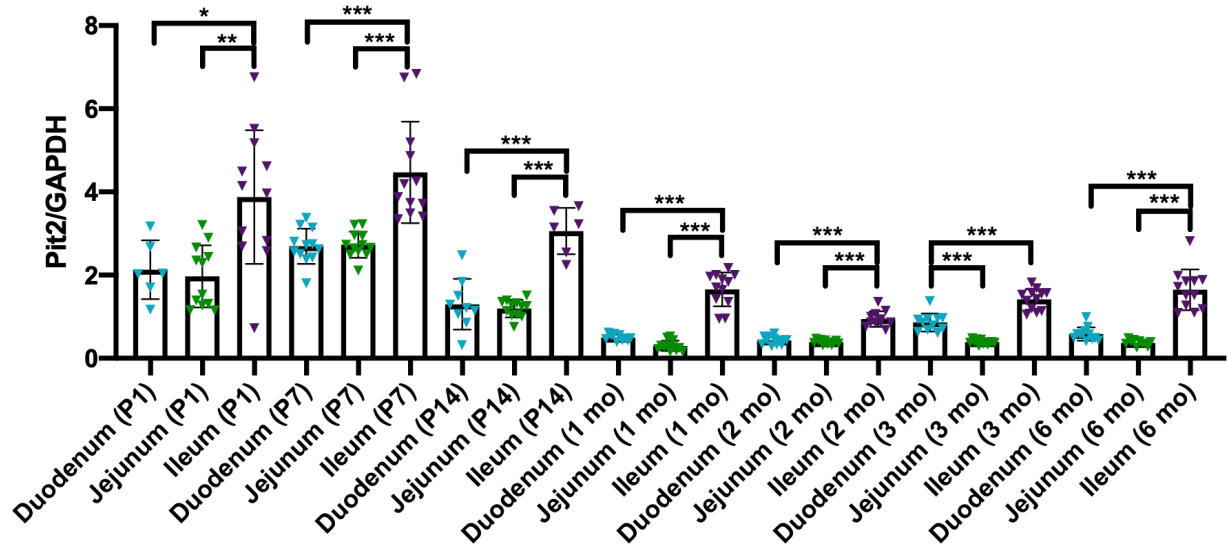


Figure 3.11. Pit2 abundance in all assessed ages and small intestine segments. Messenger RNA levels normalized to GAPDH abundance. Statistical differences between segments at each given age determined using one-way ANOVA. ($P < 0.05$).

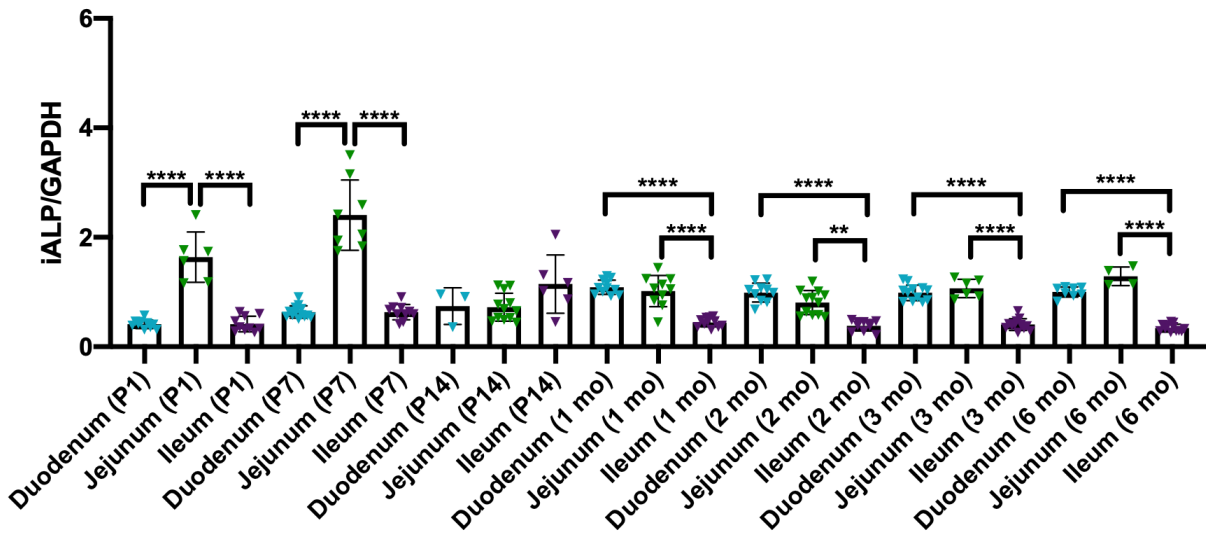


Figure 3.12. Intestinal alkaline phosphatase abundance in all studied ages and small bowel segments. Messenger RNA levels normalized to GAPDH. Statistical differences between segments in each respective age group determined using one-way ANOVA ($P < 0.05$).

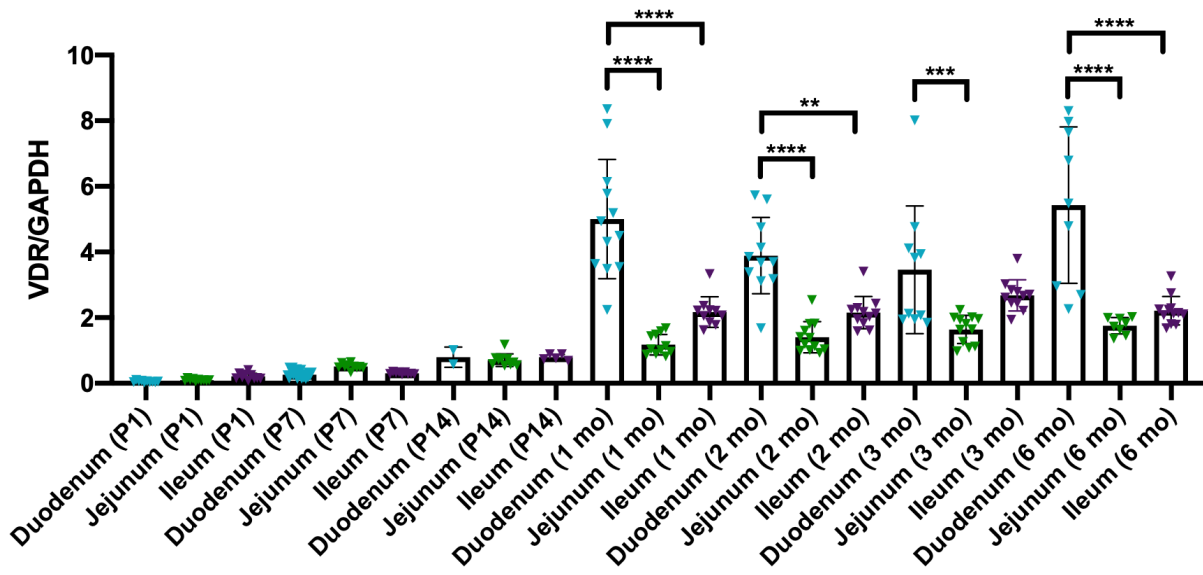


Figure 3.13. Abundance of messenger RNA encoding the vitamin D receptor across all ages and small bowel segments. Messenger RNA levels normalized to the housekeeping gene GAPDH. All statistical differences between segments at each respective age assessed using one-way ANOVA ($P < 0.05$).

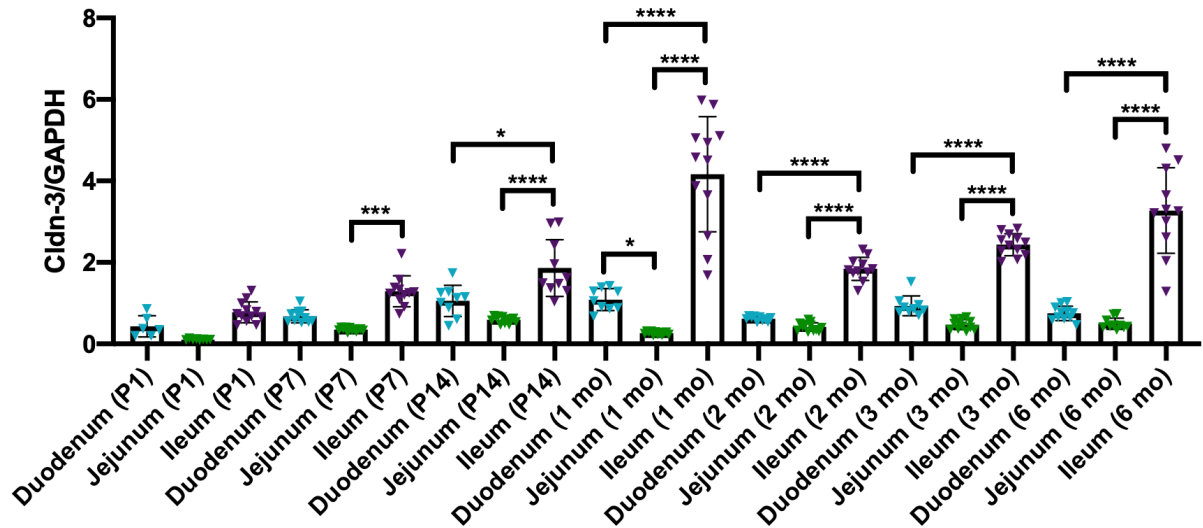


Figure 3.14. Abundance of claudin-3 messenger RNA level at all assessed ages and small bowel segments. Message abundance normalized to GAPDH. Statistical differences between small intestinal segments at each age determined using one-way ANOVA ($P < 0.05$).

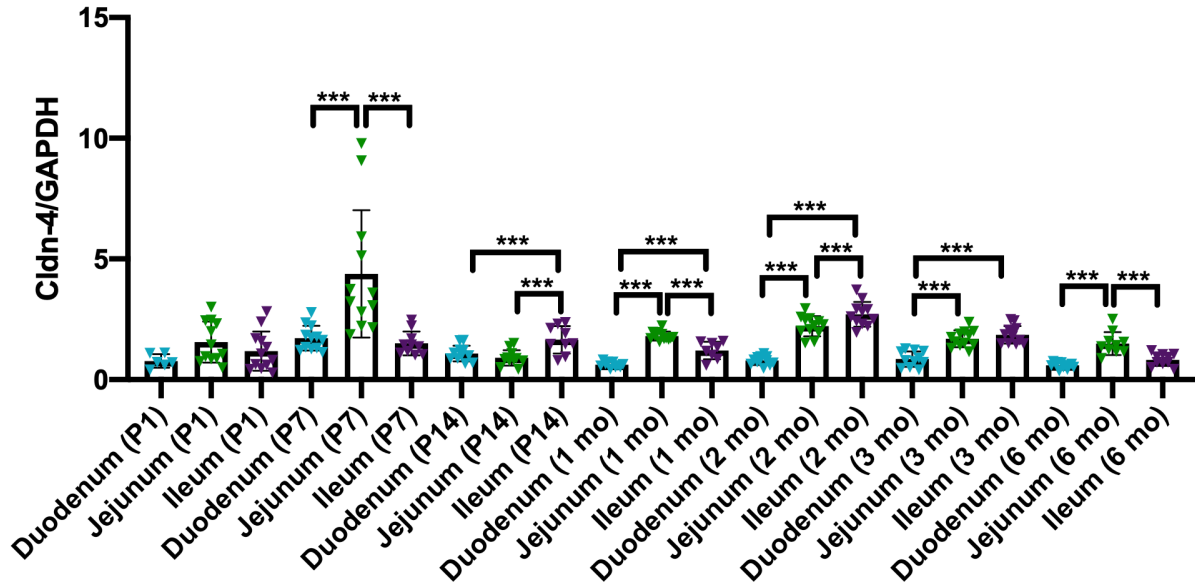


Figure 3.15. Claudin-4 messenger RNA levels in all analyzed ages and small intestine segments. mRNA abundance normalized to GAPDH. Statistical differences between segments at each age assessed using one-way ANOVA. ($P < 0.05$).

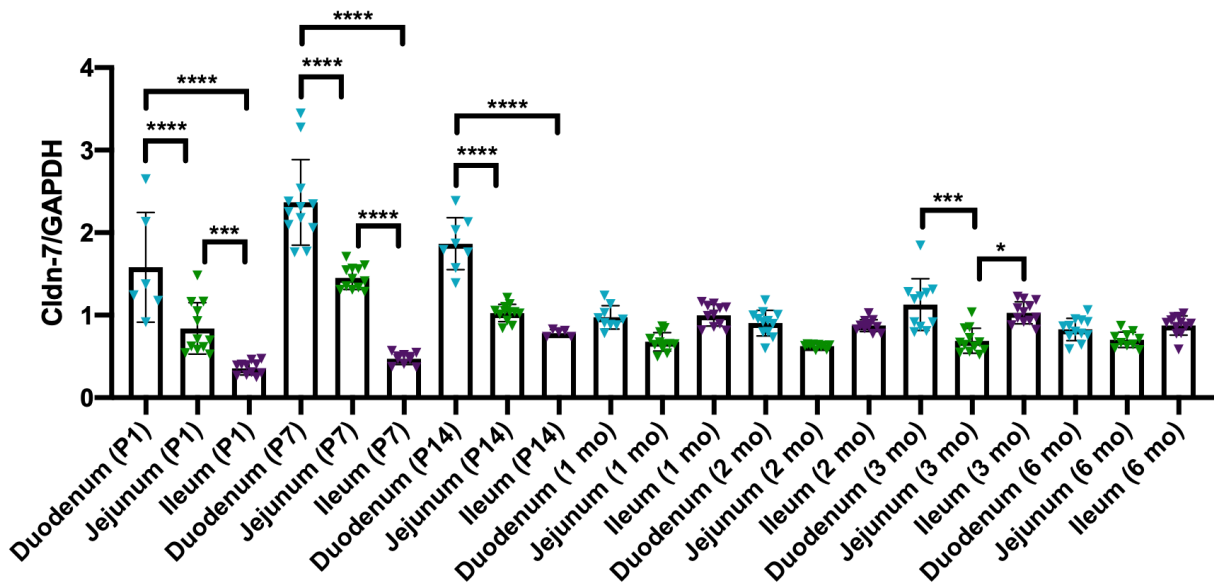


Figure 3.16. Claudin-7 message abundance across development in all small bowel segments. Messenger RNA levels normalized to that of GAPDH. Statistical differences at each age determined using one-way ANOVA ($P < 0.05$).

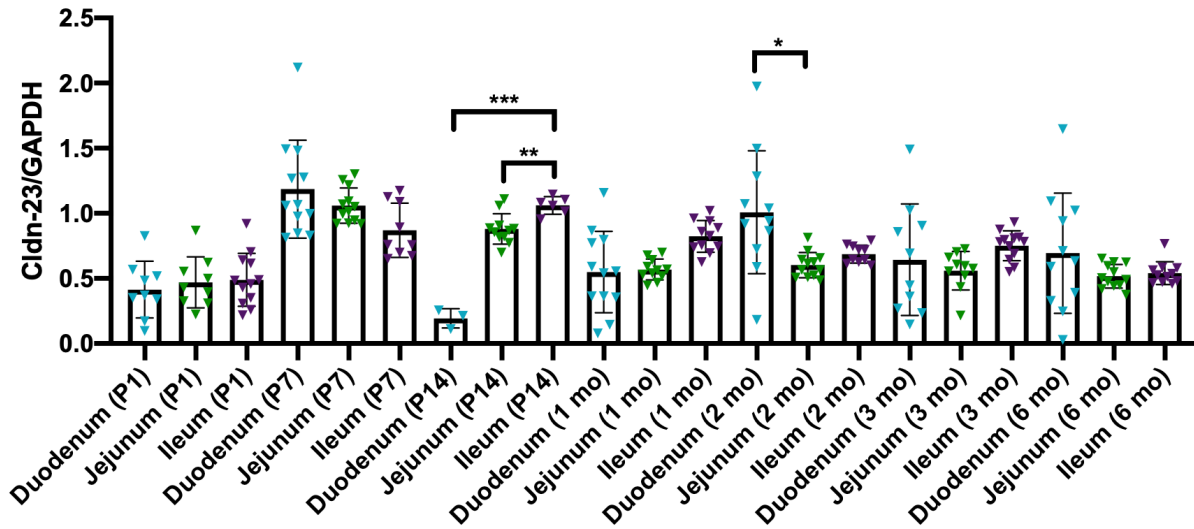


Figure 3.17. Abundance of messenger RNA encoding claudin-23 across development at each small intestine segment. Values normalized to GAPDH. Statistical differences between segments at each studied age were assessed using one-way ANOVA ($P < 0.05$).

Chapter 4 – Discussion

Intestinal Phosphate Absorption in the Young Mouse – Importance of the Transcellular and Paracellular Pathway

This study analyzes the developmental changes in phosphate absorption via both the transcellular and paracellular pathway. Given the considerably higher net transcellular phosphate flux in suckling mice relative to adults, it is evident that young mice utilize the transcellular pathway to increase phosphate absorption. The considerable difference in NaPiIIb expression at the transcript level across the small bowel between young and adult mice is a candidate to explain this functional difference. While Pit2 expression at the message level is increased early in life, its nominal role in phosphate transport leaves NaPiIIb as the likely molecular explanation for the age-dependent difference in transcellular phosphate transport. Further, the pharmacological inhibition of NaPiIIb-mediated transport in P7-P14 mice implicates the secondary active transporter in heightened transcellular phosphate absorption in young mice.

Additionally, our findings at both the functional and molecular level indicate a role of the paracellular pathway in the neonatal hyper-absorption of phosphate. Bi-ionic diffusion potential studies revealed a clear increase of paracellular phosphate permeability early in life. The difference held up both with respect to un-normalized phosphate permeability and when normalized to chloride permeability, which was itself increased early in life. This finding indicates anionic specificity with regards to phosphate permeability. Given the potential role of claudins -4 and -23 in conferring the tight junction phosphate pore, the upregulation of these claudins in the small intestine early in life may explain the increase in the significantly greater paracellular phosphate permeability in suckling mice.

Taken together, the results of this study are highly suggestive of the notion that young mammals may utilize both transcellular and paracellular transport to upregulate phosphate absorption early in life.

Phosphate Absorption in the Juvenile Animal - A Proposed Model

High urinary phosphate content combined with low expression of NaPiIIa and NaPiIIc in the first week of life are suggestive of low renal reabsorption of phosphate early in life. Given however, that serum phosphate is high at 7-14 days of age, it is likely that high intestinal phosphate absorption is compensating at the level of the small intestine. In the mammalian suckling phase, all dietary phosphate originates from breast milk. While it is understood that in human breast milk the total phosphate molarity is approximately 4 mM, the percentage breakdown between protein-bound organic phosphorus and free inorganic phosphate in breast milk is not known (83). Regardless, a notable fraction of the total phosphorus must be bound in the whey and casein protein content of breast milk, which must be enzymatically liberated by iALP prior to absorption from the lumen.

The duodenum is the most acidic segment of the small intestine given its proximity to the stomach (2). Since iALP functions optimally under basic conditions, it is plausible that organic phosphorus is liberated to a greater degree distal to the duodenum. It is important to recall however, that iALP may act both at the brush border and in the lumen upon secretion; meaning that iALP produced in duodenal enterocytes may act distal to the duodenum. Nevertheless, the transepithelial inorganic phosphate gradient is greatest in the duodenum. A 2019 study demonstrated the elevated paracellular phosphate permeability in rat small intestine at acidic pH relative to alkaline conditions (77). If this phenomenon translates to juvenile mice, the high

inorganic phosphate gradient combined with greater phosphate permeability in the acidic duodenum may translate to elevated paracellular phosphate absorption in this proximal segment. With regards to transcellular phosphate absorption in the small intestine, NaPiIIb expression is highest in the duodenum compared to the jejunum and ileum at both P1 and P7 (*Figure 3.9*). While it may be attractive to assume that this translates to the highest degree of transcellular phosphate absorption in the juvenile small bowel, it is important to remember that NaPiIIb preferentially transports the divalent (HPO_4^{2-}) over the monovalent (H_2PO_4^-) species. Since the monovalent species is predominant under the acidic conditions of the duodenum, upregulation of NaPiIIb may be a means of compensating for the suboptimal proportion of divalent phosphate to maximize the absorption of this species. Nevertheless, we propose the duodenum in the juvenile mouse to be a critical site in both paracellular and transcellular phosphate absorption.

Given that the duodenum only represents 1/9th of the length of the mouse small intestine, the transepithelial phosphate gradient may still be relatively high upon the arrival of the bolus to the jejunum. At P1 and P7 days of age, the jejunum displays the second highest NaPiIIb transcript abundance along the length of the small intestine. Additionally, conditions in the jejunum are alkaline compared to the duodenum. The consequent predominance of the divalent phosphate species in the jejunum as well as the relatively high NaPiIIb expression levels in this segment during the first week of life may well set the conditions for a high degree of transcellular phosphate absorption in the juvenile jejunum. Our functional data suggest this to be the case given the significant increase in net transcellular phosphate flux in young mice. Additionally, we have implicated NaPiIIb in this increase by blocking the transporter's function in juvenile mice *ex vivo* using NTX1942. Considering these data, we can offer reasonable conjecture that the jejunum is a critical site of transcellular phosphate absorption *in-situ*. It is also

noteworthy that paracellular phosphate permeability in the jejunum is similarly high to the duodenum in young mice, suggesting that elevated transport via the tight junction may provide an additional layer to juvenile phosphate hyperabsorption in the jejunum. As stated, local pH conditions are basic in the jejunum – This favours the activity of iALP which will continue to liberate undigested organic phosphorus bound to macromolecule sources. Thus, we propose that in the juvenile mouse, the jejunum is responsible for absorbing a high proportion of dietary phosphate via both the transcellular and paracellular pathway and is a critical site for the enzymatic liberation of phosphate from macronutrients.

In the ileum of the suckling mouse, it is quite plausible that the apical-to-basolateral phosphate gradient is considerably less pronounced than in the more proximal segments due to previous phosphate absorption during transit through the duodenum and jejunum. Thus, perhaps the remarkably high paracellular phosphate permeability in the juvenile ileum relative to the other segments reflects a mechanism to absorb the remaining ionized phosphate. It is plausible that much of the required dietary phosphate is absorbed in the duodenum and jejunum of the young mouse, and that the ileum is a site of non-energy-intensive absorption of remaining luminal phosphate. This notion would explain the relatively low NaPiIIb expression in the P1, P7 ileum compared with the duodenum and jejunum, combined with the particularly high paracellular phosphate permeability (*Figures 3.6-3.9*). The fact remains however that Slc34a2 expression in the juvenile ileum far exceeds that of the adult. Accordingly, young mice display substantially higher transcellular phosphate absorption than adult counterparts *ex vivo*, which is largely attributable to the activity of NaPiIIb at the apical membrane (*Figures 3.4, 3.5*).

It is worth noting that iALP is not consistently upregulated in young mice at the transcript level (*Figures 3.2-3.4*). This finding was contrary to our expectations, as we expected iALP

expression to be increased early in life to maximize enzymatic cleavage of phosphate from macromolecules in order to optimize phosphate absorption. To put these findings into context, it is important to consider that mice express multiple iALP splice variants (93); only the most predominant of which is shown in our results. Secondly, while it is attractive to link expression to function, this relationship may not hold true in the case of iALP. Borowitz and Granrud (1992) demonstrated that in New Zealand White Rabbits, iALP activity peaked at the juvenile stage relative to older ages in every small bowel segment (85). If this phenomenon translates to mice, the intuition to associate expression and activity may be erroneous. A third factor to consider is that iALP may act both at the brush border and in the small intestinal lumen following apical secretion by enterocytes (79). Considering this, we should note that iALP produced in a given segment of the small intestine may be secreted into the lumen and subsequently act in more distal segments.

Phosphate Absorption in the Adult Animal - A Proposed Model

A critical distinction to make between the diet composition of the suckling pups and adult mice is the source of dietary phosphate. As stated, the phosphorus in breast milk is both organic and inorganic in origin. In contrast, the phosphate content in the post-weaning diet is nearly 100% organic as it is bound largely in the 8% protein content of the PicoLab rodent diet. Therefore, in the adult small intestine, all absorbed dietary phosphate must be enzymatically cleaved from its source; namely by iALP.

The findings in this study point to a far simpler model of phosphate absorption in the adult compared to the juvenile. In both the duodenum and jejunum of the adult mouse, NaPiIIb is entirely absent at the transcript level. Since NaPiIIb is the principal player in apical phosphate

uptake, its absence in the proximal small bowel of the adult suggests a relative absence of transcellular transport and a predominance of paracellular phosphate absorption in these segments. Accordingly, our functional data in both segments display a mean net transcellular flux close to zero (*Figures 3.3, 3.4*).

In contrast to the proximal segments, the ileum is the only small intestinal segment with detectable NaPiIIb expression in the adult. Consistent with the presence of NaPiIIb, net phosphate flux values in the adult ileum display consistently positive values (*Figure 3.5*). It is reasonable to speculate that NaPiIIb is present in the distal small bowel to take up phosphate not yet absorbed in the duodenum and jejunum. Further, since paracellular phosphate permeability values are similar in the ileum to the previous two segments, we can speculate that phosphate absorption from this segment occurs via both the transcellular and paracellular routes.

The transcellular pathway is energy-intensive given the role of basolateral Na^+/K^+ ATPase in establishing the requisite gradient for apical sodium-dependent substrate uptake (94). Given that adults require a substantially lower phosphate balance than young counterparts, it is plausible that adults would conserve energy and absorb phosphate via the passive paracellular route, as appears to be the case in the adult duodenum and jejunum.

A supplementary representation of this proposed model of phosphate absorption can be found in *Figure 4.1*.

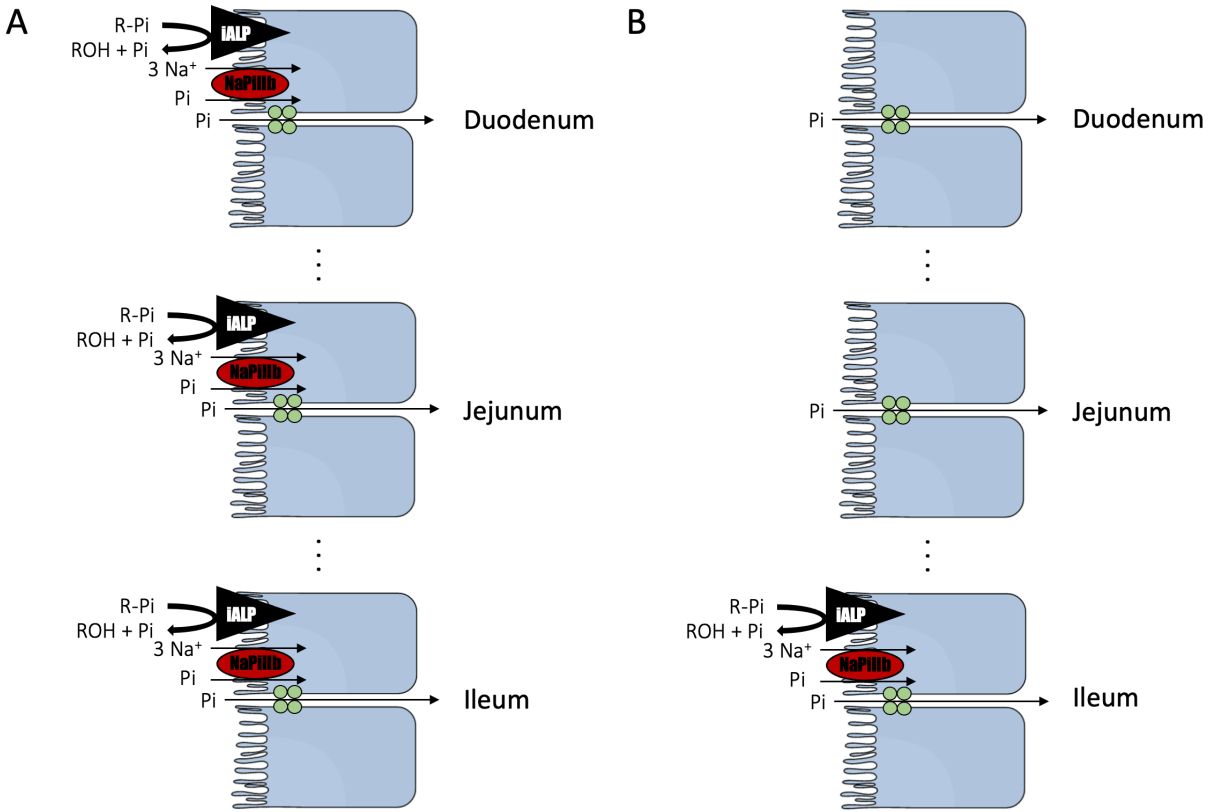


Figure 4.1. A proposed model of intestinal phosphate homeostasis in juvenile and adult mice. Displayed is a simplified model of phosphate absorption along the small intestine in A) juvenile and B) adult mice. According to this proposed model, juvenile mice hyper-absorb phosphate using a combination of transcellular and paracellular absorption along the length of the small intestine. Conversely, this model proposes that phosphate absorption in the adult is predominantly paracellular, with minimal transcellular phosphate absorption in the ileum.

Future Directions

Despite the clear lifetime peak of intestinal NaPiIIb expression early in life, the importance of NaPiIIb in establishing a positive phosphate balance in young mice remains unclear. The notion to attribute elevated juvenile phosphate absorption to increased NaPiIIb is challenged by the findings of Sabbagh et al. that intestinal-specific NaPiIIb knockout mice do not display altered serum phosphate (40). In addition, as stated previously, human mutations in NaPiIIb are not associated with a serum or urine phosphate phenotype. However, the 2009 study by Sabbagh et al. found that the NaPiIIb-null mice displayed decreased phosphate absorption which appeared to be compensated for via decreased renal phosphate excretion. This suggests that while global phosphate homeostasis may be maintained in the absence of NaPiIIb, the requirement for compensation indicates that it does indeed have a role in maintaining normal phosphate balance. It is also worth remarking that the 2009 study was performed on adult mice, in which NaPiIIb is not as instrumental to phosphate absorption as in juveniles according to our model. Thus, it should be determined whether intestinal NaPiIIb ablation in juvenile mice produces a phosphate and/or bone phenotype that may disappear or diminish with age. Further, while certain compensatory mechanisms in the absence of intestinal NaPiIIb have been established, it is not clear whether upregulation of paracellular phosphate absorption is among them. Future studies involving intestinal NaPiIIb knockout/attenuation in the small intestine of juveniles and adults should therefore study whether there exists an attendant alteration in paracellular phosphate permeability. Studies of this nature will continue to develop our understanding of the relative importance of paracellular and transcellular phosphate transport in establishing and maintaining phosphate homeostasis from infancy to adulthood. Additionally, our findings with respect to the ontogeny of NaPiIIb transcript abundance should be confirmed at

the protein level. It is also worth reiterating that this work studied one of multiple iALP splice variants. In the interest of gaining comprehensive insight into the developmental profile of iALP in the murine small intestine, additional splice variants should be analyzed in future work.

While we have provided grounds for speculation as to why claudins -4 and -23 may confer the paracellular phosphate pore, future work must be done investigating the role of these claudins in phosphate permeability. Principal findings with regards to roles of specific claudins in ion flux are often found using either overexpression or ablation (E.g. RNA interference) approaches in cell monolayer models (78, 95). Following investigation in cell models of whether claudins -4 and -23 influence phosphate flux through the tight junction, intestinal-specific knockouts of these claudins may be generated to determine their respective or complimentary roles in phosphate homeostasis.

References

1. **Peacock M.** Phosphate Metabolism in Health and Disease. *Calcif Tissue Int* 108: 3–15, 2021. doi: 10.1007/s00223-020-00686-3.
2. **Evans D, Pye G, Clark A, Dyson T, Hardcastle J.** Measurement of gastrointestinal pH profiles in normal ambulant human subjects. 29: 1035–1041, 1988.
3. **Greenberg BG, Winters RW, Graham JB.** The normal range of serum inorganic phosphorus and its utility as a discriminant in the diagnosis of congenital hypophosphatemia. *J Clin Endocrinol Metab* 20: 364–79, 1960. doi: 10.1210/jcem-20-3-364.
4. **Stearns G; W.** Studies of phosphorus of blood. 1. The partition of phosphorus in whole blood and serum, the serum calcium and plasma phosphatase from birth to maturity. *Journal of Biological Chemistry* 102, 1933.
5. **Amanzadeh J, Reilly RF.** Hypophosphatemia: an evidence-based approach to its clinical consequences and management. *Nat Clin Pract Nephrol* 2: 136–48, 2006. doi: 10.1038/ncpneph0124.
6. **Iheagwara OS, Ing TS, Kjellstrand CM, Lew SQ.** Phosphorus, phosphorous, and phosphate. *Hemodial Int* 17: 479–82, 2013. doi: 10.1111/hdi.12010.
7. **Ferrari SL, Bonjour JP, Rizzoli R.** Fibroblast growth factor-23 relationship to dietary phosphate and renal phosphate handling in healthy young men. *J Clin Endocrinol Metab* 90: 1519–24, 2005. doi: 10.1210/jc.2004-1039.
8. **Layunta E, Pastor Arroyo EM, Kagi L, Thomas L, Levi M, Hernando N, Wagner CA.** Intestinal Response to Acute Intra-gastric and Intravenous Administration of Phosphate in Rats. *Cell Physiol Biochem* 52: 838–849, 2019. doi: 10.33594/000000058.
9. **Takashi Y, Kosako H, Sawatsubashi S, Kinoshita Y, Ito N, Tsoumpra MK, Nangaku M, Abe M, Matsuhisa M, Kato S, Matsumoto T, Fukumoto S.** Activation of unliganded FGF receptor by extracellular phosphate potentiates proteolytic protection of FGF23 by its O-glycosylation. *Proc Natl Acad Sci USA* 116: 11418–11427, 2019. doi: 10.1073/pnas.1815166116.
10. **Hernando N, Pastor-Arroyo EM, Marks J, Schnitzbauer U, Knopfel T, Burki M, Bettoni C, Wagner CA.** 1,25(OH)₂ vitamin D₃ stimulates active phosphate transport but not paracellular phosphate absorption in mouse intestine. *J Physiol* 599: 1131–1150, 2021. doi: 10.1113/JP280345.
11. **Xu H, Bai L, Collins JF, Ghishan FK.** Age-dependent regulation of rat intestinal type IIb sodium-phosphate cotransporter by 1,25-(OH)₂ vitamin D₃. *Am J Physiol Cell Physiol* 282: C487-93, 2002. doi: 10.1152/ajpcell.00412.2001.

12. **Schlemmer U, Frolich W, Prieto RM, Grases F.** Phytate in foods and significance for humans: food sources, intake, processing, bioavailability, protective role and analysis. *Mol Nutr Food Res* 53 Suppl 2: S330-75, 2009. doi: 10.1002/mnfr.200900099.
13. **Bai W, Li J, Liu J.** Serum phosphorus, cardiovascular and all-cause mortality in the general population: A meta-analysis. *Clin Chim Acta* 461: 76–82, 2016. doi: 10.1016/j.cca.2016.07.020.
14. **Sim JJ, Bhandari SK, Smith N, Chung J, Liu IL, Jacobsen SJ, Kalantar-Zadeh K.** Phosphorus and risk of renal failure in subjects with normal renal function. *Am J Med* 126: 311–8, 2013. doi: 10.1016/j.amjmed.2012.08.018.
15. **Beck-Nielsen SS, Brock-Jacobsen B, Gram J, Brixen K, Jensen TK.** Incidence and prevalence of nutritional and hereditary rickets in southern Denmark. *Eur J Endocrinol* 160: 491–7, 2009. doi: 10.1530/EJE-08-0818.
16. **Rafaelsen S, Johansson S, Raeder H, Bjerknes R.** Hereditary hypophosphatemia in Norway: a retrospective population-based study of genotypes, phenotypes, and treatment complications. *Eur J Endocrinol* 174: 125–36, 2016. doi: 10.1530/EJE-15-0515.
17. **Mameli C, Sangiorgio A, Colombo V, Gambino M, Spaccini L, Cattaneo E, Zuccotti GV.** Autosomal Dominant Hypophosphatemic Rickets: A Case Report and Review of the Literature. *Int J Environ Res Public Health* 18, 2021. doi: 10.3390/ijerph18168771.
18. **Levy-Litan V, Hershkovitz E, Avizov L, Leventhal N, Bercovich D, Chalifa-Caspi V, Manor E, Buriakovsky S, Hadad Y, Goding J, Parvari R.** Autosomal-recessive hypophosphatemic rickets is associated with an inactivation mutation in the ENPP1 gene. *Am J Hum Genet* 86: 273–8, 2010. doi: 10.1016/j.ajhg.2010.01.010.
19. **Bailey DA, McKay HA, Mirwald RL, Crocker PR, Faulkner RA.** A six-year longitudinal study of the relationship of physical activity to bone mineral accrual in growing children: the university of Saskatchewan bone mineral accrual study. *J Bone Miner Res* 14: 1672–9, 1999. doi: 10.1359/jbmr.1999.14.10.1672.
20. **Davies JH, Evans BA, Gregory JW.** Bone mass acquisition in healthy children. *Arch Dis Child* 90: 373–8, 2005. doi: 10.1136/adc.2004.053553.
21. **Wubuli A, Reyer H, Murani E, Ponsuksili S, Wolf P, Oster M, Wimmers K.** Tissue-Wide Gene Expression Analysis of Sodium/Phosphate Co-Transporters in Pigs. *Int J Mol Sci* 20, 2019. doi: 10.3390/ijms20225576.
22. **Madjdpour C, Bacic D, Kaissling B, Murer H, Biber J.** Segment-specific expression of sodium-phosphate cotransporters NaPi-IIa and -IIc and interacting proteins in mouse renal proximal tubules. *Pflugers Arch* 448: 402–10, 2004. doi: 10.1007/s00424-004-1253-x.
23. **Gattineni J, Twombly K, Goetz R, Mohammadi M, Baum M.** Regulation of serum 1,25(OH)₂ vitamin D₃ levels by fibroblast growth factor 23 is mediated by FGF receptors 3 and 4. *Am J Physiol Renal Physiol* 301: F371-7, 2011. doi: 10.1152/ajprenal.00740.2010.

24. **Virkki LV, Forster IC, Biber J, Murer H.** Substrate interactions in the human type IIa sodium-phosphate cotransporter (NaPi-IIa). *Am J Physiol Renal Physiol* 288: F969-81, 2005. doi: 10.1152/ajprenal.00293.2004.
25. **Forster IC, Kohler K, Biber J, Murer H.** Forging the link between structure and function of electrogenic cotransporters: the renal type IIa Na⁺/Pi cotransporter as a case study. *Prog Biophys Mol Biol* 80: 69–108, 2002. doi: 10.1016/s0079-6107(02)00015-9.
26. **Fenollar-Ferrer C, Patti M, Knopfel T, Werner A, Forster IC, Forrest LR.** Structural fold and binding sites of the human Na⁽⁺⁾-phosphate cotransporter NaPi-II. *Biophys J* 106: 1268–79, 2014. doi: 10.1016/j.bpj.2014.01.043.
27. **Kohler K, Forster IC, Lambert G, Biber J, Murer H.** The functional unit of the renal type IIa Na⁺/Pi cotransporter is a monomer. *J Biol Chem* 275: 26113–20, 2000. doi: 10.1074/jbc.M003564200.
28. **Oddsson A, Sulem P, Helgason H, Edvardsson VO, Thorleifsson G, Sveinbjornsson G, Haraldsdottir E, Eyjolfsson GI, Sigurdardottir O, Olafsson I, Masson G, Holm H, Gudbjartsson DF, Thorsteinsdottir U, Indridason OS, Palsson R, Stefansson K.** Common and rare variants associated with kidney stones and biochemical traits. *Nat Commun* 6: 7975, 2015. doi: 10.1038/ncomms8975.
29. **Prie D, Huart V, Bakouh N, Planelles G, Dellis O, Gerard B, Hulin P, Benque-Blanchet F, Silve C, Grandchamp B, Friedlander G.** Nephrolithiasis and osteoporosis associated with hypophosphatemia caused by mutations in the type 2a sodium-phosphate cotransporter. *N Engl J Med* 347: 983–91, 2002. doi: 10.1056/NEJMoa020028.
30. **Rajagopal A, Braslavsky D, Lu JT, Kleppe S, Clement F, Cassinelli H, Liu DS, Liern JM, Vallejo G, Bergada I, Gibbs RA, Campeau PM, Lee BH.** Exome sequencing identifies a novel homozygous mutation in the phosphate transporter SLC34A1 in hypophosphatemia and nephrocalcinosis. *J Clin Endocrinol Metab* 99: E2451-6, 2014. doi: 10.1210/jc.2014-1517.
31. **Braun DA, Lawson JA, Gee HY, Halbritter J, Shril S, Tan W, Stein D, Wassner AJ, Ferguson MA, Gucev Z, Fisher B, Spaneas L, Varner J, Sayer JA, Milosevic D, Baum M, Tasic V, Hildebrandt F.** Prevalence of Monogenic Causes in Pediatric Patients with Nephrolithiasis or Nephrocalcinosis. *Clin J Am Soc Nephrol* 11: 664–72, 2016. doi: 10.2215/CJN.07540715.
32. **Halbritter J, Baum M, Hynes AM, Rice SJ, Thwaites DT, Gucev ZS, Fisher B, Spaneas L, Porath JD, Braun DA, Wassner AJ, Nelson CP, Tasic V, Sayer JA, Hildebrandt F.** Fourteen monogenic genes account for 15% of nephrolithiasis/nephrocalcinosis. *J Am Soc Nephrol* 26: 543–51, 2015. doi: 10.1681/ASN.2014040388.
33. **Dinour D, Davidovits M, Ganon L, Ruminska J, Forster IC, Hernando N, Eyal E, Holtzman EJ, Wagner CA.** Loss of function of NaPiIIa causes nephrocalcinosis and possibly kidney insufficiency. *Pediatr Nephrol* 31: 2289–2297, 2016. doi: 10.1007/s00467-016-3443-0.

34. **Hureaux M, Molin A, Jay N, Saliou AH, Spaggiari E, Salomon R, Benachi A, Vargas-Poussou R, Heidet L.** Prenatal hyperechogenic kidneys in three cases of infantile hypercalcemia associated with SLC34A1 mutations. *Pediatr Nephrol* 33: 1723–1729, 2018. doi: 10.1007/s00467-018-3998-z.
35. **Pronicka E, Ciara E, Halat P, Janiec A, Wojcik M, Rowinska E, Rokicki D, Pludowski P, Wojciechowska E, Wierzbicka A, Ksiazek JB, Jacoszek A, Konrad M, Schlingmann KP, Litwin M.** Biallelic mutations in CYP24A1 or SLC34A1 as a cause of infantile idiopathic hypercalcemia (IIH) with vitamin D hypersensitivity: molecular study of 11 historical IIH cases. *J Appl Genet* 58: 349–353, 2017. doi: 10.1007/s13353-017-0397-2.
36. **Schlingmann KP, Ruminska J, Kaufmann M, Dursun I, Patti M, Kranz B, Pronicka E, Ciara E, Akcay T, Bulus D, Cornelissen EA, Gawlik A, Sikora P, Patzer L, Galiano M, Boyadzhiev V, Dumic M, Vivante A, Kleta R, Dekel B, Levtchenko E, Bindels RJ, Rust S, Forster IC, Hernando N, Jones G, Wagner CA, Konrad M.** Autosomal-Recessive Mutations in SLC34A1 Encoding Sodium-Phosphate Cotransporter 2A Cause Idiopathic Infantile Hypercalcemia. *J Am Soc Nephrol* 27: 604–14, 2016. doi: 10.1681/ASN.2014101025.
37. **Levi M, Gratton E, Forster IC, Hernando N, Wagner CA, Biber J, Sorribas V, Murer H.** Mechanisms of phosphate transport. *Nat Rev Nephrol* 15: 482–500, 2019. doi: 10.1038/s41581-019-0159-y.
38. **Beck L, Karaplis AC, Amizuka N, Hewson AS, Ozawa H, Tenenhouse HS.** Targeted inactivation of Npt2 in mice leads to severe renal phosphate wasting, hypercalciuria, and skeletal abnormalities. *Proc Natl Acad Sci U S A* 95: 5372–7, 1998. doi: 10.1073/pnas.95.9.5372.
39. **Thomas L, Xue J, Murali SK, Fenton RA, Dominguez Rieg JA, Rieg T.** Pharmacological Npt2a Inhibition Causes Phosphaturia and Reduces Plasma Phosphate in Mice with Normal and Reduced Kidney Function. *J Am Soc Nephrol* 30: 2128–2139, 2019. doi: 10.1681/ASN.2018121250.
40. **Sabbagh Y, O'Brien SP, Song W, Boulanger JH, Stockmann A, Arbeeny C, Schiavi SC.** Intestinal npt2b plays a major role in phosphate absorption and homeostasis. *J Am Soc Nephrol* 20: 2348–58, 2009. doi: 10.1681/ASN.2009050559.
41. **Traebert M, Hattenhauer O, Murer H, Kaissling B, Biber J.** Expression of type II Na-P(i) cotransporter in alveolar type II cells. *Am J Physiol* 277: L868-73, 1999. doi: 10.1152/ajplung.1999.277.5.L868.
42. **Motta SE, Imenez Silva PH, Daryadel A, Haykir B, Pastor-Arroyo EM, Bettoni C, Hernando N, Wagner CA.** Expression of NaPi-IIb in rodent and human kidney and upregulation in a model of chronic kidney disease. *Pflugers Arch* 472: 449–460, 2020. doi: 10.1007/s00424-020-02370-9.
43. **Gryshkova V, Lituiev D, Savinska L, Ovcharenko G, Gout I, Filonenko V, Kiyamova R.** Generation of monoclonal antibodies against tumor-associated antigen MX35/sodium-

- dependent phosphate transporter NaPi2b. *Hybridoma (Larchmt)* 30: 37–42, 2011. doi: 10.1089/hyb.2010.0064.
44. **Giral H, Cranston D, Lanzano L, Caldas Y, Sutherland E, Rachelson J, Dobrinskikh E, Weinman EJ, Doctor RB, Gratton E, Levi M.** NHE3 regulatory factor 1 (NHERF1) modulates intestinal sodium-dependent phosphate transporter (NaPi-2b) expression in apical microvilli. *J Biol Chem* 287: 35047–35056, 2012. doi: 10.1074/jbc.M112.392415.
 45. **Huber K, Muscher A, Breves G.** Sodium-dependent phosphate transport across the apical membrane of alveolar epithelium in caprine mammary gland. *Comp Biochem Physiol A Mol Integr Physiol* 146: 215–22, 2007. doi: 10.1016/j.cbpa.2006.10.024.
 46. **Marks J, Srail SK, Biber J, Murer H, Unwin RJ, Debnam ES.** Intestinal phosphate absorption and the effect of vitamin D: a comparison of rats with mice. *Exp Physiol* 91: 531–7, 2006. doi: 10.1113/expphysiol.2005.032516.
 47. **Radanovic T, Wagner CA, Murer H, Biber J.** Regulation of intestinal phosphate transport. I. Segmental expression and adaptation to low-P(i) diet of the type IIb Na(+)-P(i) cotransporter in mouse small intestine. *Am J Physiol Gastrointest Liver Physiol* 288: G496–500, 2005. doi: 10.1152/ajpgi.00167.2004.
 48. **Corut A, Senyigit A, Ugur SA, Altin S, Ozcelik U, Calisir H, Yildirim Z, Gocmen A, Tolun A.** Mutations in SLC34A2 cause pulmonary alveolar microlithiasis and are possibly associated with testicular microlithiasis. *Am J Hum Genet* 79: 650–6, 2006. doi: 10.1086/508263.
 49. **Ohi A, Hanabusa E, Ueda O, Segawa H, Horiba N, Kaneko I, Kuwahara S, Mukai T, Sasaki S, Tominaga R, Furutani J, Aranami F, Ohtomo S, Oikawa Y, Kawase Y, Wada NA, Tachibe T, Kakefuda M, Tateishi H, Matsumoto K, Tatsumi S, Kido S, Fukushima N, Jishage K, Miyamoto K.** Inorganic phosphate homeostasis in sodium-dependent phosphate cotransporter Npt2b(+)/(-) mice. *Am J Physiol Renal Physiol* 301: F1105–13, 2011. doi: 10.1152/ajprenal.00663.2010.
 50. **Larsson TE, Kameoka C, Nakajo I, Taniuchi Y, Yoshida S, Akizawa T, Smulders RA.** NPT-IIb Inhibition Does Not Improve Hyperphosphatemia in CKD. *Kidney Int Rep* 3: 73–80, 2018. doi: 10.1016/j.ekir.2017.08.003.
 51. **Becker BN, Schulman G.** Nephrotoxicity of antiviral therapies. *Curr Opin Nephrol Hypertens* 5: 375–9, 1996. doi: 10.1097/00041552-199607000-00015.
 52. **Segawa H, Kaneko I, Takahashi A, Kuwahata M, Ito M, Ohkido I, Tatsumi S, Miyamoto K.** Growth-related renal type II Na/Pi cotransporter. *J Biol Chem* 277: 19665–72, 2002. doi: 10.1074/jbc.M200943200.
 53. **Picard N, Capuano P, Stange G, Mihailova M, Kaissling B, Murer H, Biber J, Wagner CA.** Acute parathyroid hormone differentially regulates renal brush border membrane phosphate cotransporters. *Pflugers Arch* 460: 677–87, 2010. doi: 10.1007/s00424-010-0841-1.

54. **Bergwitz C, Miyamoto KI.** Hereditary hypophosphatemic rickets with hypercalciuria: pathophysiology, clinical presentation, diagnosis and therapy. *Pflugers Arch* 471: 149–163, 2019. doi: 10.1007/s00424-018-2184-2.
55. **Colazo JM, Reasoner SA, Holt G, Faugere MCM, Dahir KM.** Hereditary Hypophosphatemic Rickets with Hypercalciuria (HHRH) Presenting with Genu Valgum Deformity: Treatment with Phosphate Supplementation and Surgical Correction. *Case Rep Endocrinol* 2020: 1047327, 2020. doi: 10.1155/2020/1047327.
56. **Myakala K, Motta S, Murer H, Wagner CA, Koesters R, Biber J, Hernando N.** Renal-specific and inducible depletion of NaPi-IIc/Slc34a3, the cotransporter mutated in HHRH, does not affect phosphate or calcium homeostasis in mice. *Am J Physiol Renal Physiol* 306: F833-43, 2014. doi: 10.1152/ajprenal.00133.2013.
57. **Kavanaugh MP, Kabat D.** Identification and characterization of a widely expressed phosphate transporter/retrovirus receptor family. *Kidney Int* 49: 959–63, 1996. doi: 10.1038/ki.1996.135.
58. **Bon N, Couasnay G, Bourguine A, Sourice S, Beck-Cormier S, Guicheux J, Beck L.** Phosphate (Pi)-regulated heterodimerization of the high-affinity sodium-dependent Pi transporters PiT1/Slc20a1 and PiT2/Slc20a2 underlies extracellular Pi sensing independently of Pi uptake. *J Biol Chem* 293: 2102–2114, 2018. doi: 10.1074/jbc.M117.807339.
59. **Beck L, Leroy C, Beck-Cormier S, Forand A, Salaun C, Paris N, Bernier A, Urena-Torres P, Prie D, Ollero M, Coulombel L, Friedlander G.** The phosphate transporter PiT1 (Slc20a1) revealed as a new essential gene for mouse liver development. *PLoS One* 5: e9148, 2010. doi: 10.1371/journal.pone.0009148.
60. **Zoidis E, Ghirlanda-Keller C, Gosteli-Peter M, Zapf J, Schmid C.** Regulation of phosphate (Pi) transport and NaPi-III transporter (Pit-1) mRNA in rat osteoblasts. *J Endocrinol* 181: 531–40, 2004. doi: 10.1677/joe.0.1810531.
61. **Villa-Bellosta R, Ravera S, Sorribas V, Stange G, Levi M, Murer H, Biber J, Forster IC.** The Na⁺-Pi cotransporter PiT-2 (SLC20A2) is expressed in the apical membrane of rat renal proximal tubules and regulated by dietary Pi. *Am J Physiol Renal Physiol* 296: F691-9, 2009. doi: 10.1152/ajprenal.90623.2008.
62. **Pastor-Arroyo EM, Knopfel T, Imenez Silva PH, Schnitzbauer U, Poncet N, Biber J, Wagner CA, Hernando N.** Intestinal epithelial ablation of Pit-2/Slc20a2 in mice leads to sustained elevation of vitamin D3 upon dietary restriction of phosphate. *Acta Physiol (Oxf)* 230: e13526, 2020. doi: 10.1111/apha.13526.
63. **Wang C, Li Y, Shi L, Ren J, Patti M, Wang T, de Oliveira JR, Sobrido MJ, Quintans B, Baquero M, Cui X, Zhang XY, Wang L, Xu H, Wang J, Yao J, Dai X, Liu J, Zhang L, Ma H, Gao Y, Ma X, Feng S, Liu M, Wang QK, Forster IC, Zhang X, Liu JY.** Mutations in SLC20A2 link familial idiopathic basal ganglia calcification with phosphate homeostasis. *Nat Genet* 44: 254–6, 2012. doi: 10.1038/ng.1077.

64. **Sabbagh Y, Giral H, Caldas Y, Levi M, Schiavi SC.** Intestinal phosphate transport. *Adv Chronic Kidney Dis* 18: 85–90, 2011. doi: 10.1053/j.ackd.2010.11.004.
65. **Davis GR, Zerwekh JE, Parker TF, Krejs GJ, Pak CY, Fordtran JS.** Absorption of phosphate in the jejunum of patients with chronic renal failure before and after correction of vitamin D deficiency. *Gastroenterology* 85: 908–16, 1983.
66. **King AJ, Siegel M, He Y, Nie B, Wang J, Koo-McCoy S, Minassian NA, Jafri Q, Pan D, Kohler J, Kumaraswamy P, Kozuka K, Lewis JG, Dragoli D, Rosenbaum DP, O'Neill D, Plain A, Greasley PJ, Jonsson-Rylander AC, Karlsson D, Behrendt M, Stromstedt M, Ryden-Bergsten T, Knopfel T, Pastor Arroyo EM, Hernando N, Marks J, Donowitz M, Wagner CA, Alexander RT, Caldwell JS.** Inhibition of sodium/hydrogen exchanger 3 in the gastrointestinal tract by tenapanor reduces paracellular phosphate permeability. *Sci Transl Med* 10, 2018. doi: 10.1126/scitranslmed.aam6474.
67. **Block GA, Rosenbaum DP, Leonsson-Zachrisson M, Astrand M, Johansson S, Knutsson M, Langkilde AM, Chertow GM.** Effect of Tenapanor on Serum Phosphate in Patients Receiving Hemodialysis. *J Am Soc Nephrol* 28: 1933–1942, 2017. doi: 10.1681/ASN.2016080855.
68. **Katoh M, Katoh M.** CLDN23 gene, frequently down-regulated in intestinal-type gastric cancer, is a novel member of CLAUDIN gene family. *Int J Mol Med* 11: 683–9, 2003.
69. **Achari C, Winslow S, Larsson C.** Down Regulation of CLDN1 Induces Apoptosis in Breast Cancer Cells. *PLoS One* 10: e0130300, 2015. doi: 10.1371/journal.pone.0130300.
70. **Bhat AA, Pope JL, Smith JJ, Ahmad R, Chen X, Washington MK, Beauchamp RD, Singh AB, Dhawan P.** Claudin-7 expression induces mesenchymal to epithelial transformation (MET) to inhibit colon tumorigenesis. *Oncogene* 34: 4570–80, 2015. doi: 10.1038/onc.2014.385.
71. **Tsukita S, Tanaka H, Tamura A.** The Claudins: From Tight Junctions to Biological Systems. *Trends Biochem Sci* 44: 141–152, 2019. doi: 10.1016/j.tibs.2018.09.008.
72. **Anderson JM, Van Itallie CM.** Physiology and function of the tight junction. *Cold Spring Harb Perspect Biol* 1: a002584, 2009. doi: 10.1101/cshperspect.a002584.
73. **Ikari A, Hirai N, Shiroma M, Harada H, Sakai H, Hayashi H, Suzuki Y, Degawa M, Takagi K.** Association of paracellin-1 with ZO-1 augments the reabsorption of divalent cations in renal epithelial cells. *J Biol Chem* 279: 54826–32, 2004. doi: 10.1074/jbc.M406331200.
74. **Hou J, Shan Q, Wang T, Gomes AS, Yan Q, Paul DL, Bleich M, Goodenough DA.** Transgenic RNAi depletion of claudin-16 and the renal handling of magnesium. *J Biol Chem* 282: 17114–22, 2007. doi: 10.1074/jbc.M700632200.

75. **Hou J, Renigunta A, Konrad M, Gomes AS, Schneeberger EE, Paul DL, Waldegger S, Goodenough DA.** Claudin-16 and claudin-19 interact and form a cation-selective tight junction complex. *J Clin Invest* 118: 619–28, 2008. doi: 10.1172/JCI33970.
76. **Mineta K, Yamamoto Y, Yamazaki Y, Tanaka H, Tada Y, Saito K, Tamura A, Igarashi M, Endo T, Takeuchi K, Tsukita S.** Predicted expansion of the claudin multigene family. *FEBS Lett* 585: 606–12, 2011. doi: 10.1016/j.febslet.2011.01.028.
77. **Knopfel T, Himmerkus N, Gunzel D, Bleich M, Hernando N, Wagner CA.** Paracellular transport of phosphate along the intestine. *Am J Physiol Gastrointest Liver Physiol* 317: G233–G241, 2019. doi: 10.1152/ajpgi.00032.2019.
78. **Hou J, Renigunta A, Yang J, Waldegger S.** Claudin-4 forms paracellular chloride channel in the kidney and requires claudin-8 for tight junction localization. *Proc Natl Acad Sci U S A* 107: 18010–5, 2010. doi: 10.1073/pnas.1009399107.
79. **Eliakim R, Mahmood A, Alpers DH.** Rat intestinal alkaline phosphatase secretion into lumen and serum is coordinately regulated. *Biochim Biophys Acta* 1091: 1–8, 1991. doi: 10.1016/0167-4889(91)90213-h.
80. **Namikawa T, Ishida N, Tsuda S, Fujisawa K, Munekage E, Iwabu J, Munekage M, Uemura S, Tsujii S, Tamura T, Yatabe T, Maeda H, Kitagawa H, Kobayashi M, Hanazaki K.** Prognostic significance of serum alkaline phosphatase and lactate dehydrogenase levels in patients with unresectable advanced gastric cancer. *Gastric Cancer* 22: 684–691, 2019. doi: 10.1007/s10120-018-0897-8.
81. **Belkhouribchia J, Bravenboer B, Meuwissen M, Velkeniers B.** Osteomalacia with low alkaline phosphatase: a not so rare condition with important consequences. *BMJ Case Rep* 2016, 2016. doi: 10.1136/bcr-2015-212827.
82. **Cupisti A, Kalantar-Zadeh K.** Management of natural and added dietary phosphorus burden in kidney disease. *Semin Nephrol* 33: 180–90, 2013. doi: 10.1016/j.semnephrol.2012.12.018.
83. **Nickkho-Amiry M, Prentice A, Ledi F, Laskey MA, Das G, Berry JL, Mughal MZ.** Maternal vitamin D status and breast milk concentrations of calcium and phosphorus. *Arch Dis Child* 93: 179, 2008. doi: 10.1136/adc.2007.124008.
84. **Vorland CJ, Lachcik PJ, Aromeh LO, Moe SM, Chen NX, Hill Gallant KM.** Effect of dietary phosphorus intake and age on intestinal phosphorus absorption efficiency and phosphorus balance in male rats. *PLoS One* 13: e0207601, 2018. doi: 10.1371/journal.pone.0207601.
85. **Borowitz SM, Granrud GS.** Ontogeny of intestinal phosphate absorption in rabbits. *Am J Physiol* 262: G847-53, 1992. doi: 10.1152/ajpgi.1992.262.5.G847.

86. **Bistarakis L, Voskaki I, Lambadaridis J, Sereti H, Sbyrakis S.** Renal handling of phosphate in the first six months of life. *Arch Dis Child* 61: 677–81, 1986. doi: 10.1136/adc.61.7.677.
87. **Kaskel FJ, Kumar AM, Feld LG, Spitzer A.** Renal reabsorption of phosphate during development: tubular events. *Pediatr Nephrol* 2: 129–34, 1988. doi: 10.1007/BF00870393.
88. **Neiberger RE, Barac-Nieto M, Spitzer A.** Renal reabsorption of phosphate during development: transport kinetics in BBMV. *Am J Physiol* 257: F268-74, 1989. doi: 10.1152/ajprenal.1989.257.2.F268.
89. **Beggs MR, Appel I, Svenningsen P, Skjodt K, Alexander RT, Dimke H.** Expression of transcellular and paracellular calcium and magnesium transport proteins in renal and intestinal epithelia during lactation. *Am J Physiol Renal Physiol* 313: F629–F640, 2017. doi: 10.1152/ajprenal.00680.2016.
90. **Rievaj J, Pan W, Cordat E, Alexander RT.** The Na(+)/H(+) exchanger isoform 3 is required for active paracellular and transcellular Ca(2)(+) transport across murine cecum. *Am J Physiol Gastrointest Liver Physiol* 305: G303-13, 2013. doi: 10.1152/ajpgi.00490.2012.
91. **Kimizuka H, Koketsu K.** Ion transport through cell membrane. *J Theor Biol* 6: 290–305, 1964. doi: 10.1016/0022-5193(64)90035-9.
92. **Navre M, Labonte E, Carreras C.** Novel Non-Systemic NaP2b Inhibitors Block Intestinal Phosphate Uptake. , 2011.
93. **Noda S, Yamada A, Nakaoka K, Goseki-Sone M.** 1-alpha,25-Dihydroxyvitamin D3 up-regulates the expression of 2 types of human intestinal alkaline phosphatase alternative splicing variants in Caco-2 cells and may be an important regulator of their expression in gut homeostasis. *Nutr Res* 46: 59–67, 2017. doi: 10.1016/j.nutres.2017.07.005.
94. **Thorsen K, Drengstig T, Ruoff P.** Transepithelial glucose transport and Na⁺/K⁺ homeostasis in enterocytes: an integrative model. *Am J Physiol Cell Physiol* 307: C320-37, 2014. doi: 10.1152/ajpcell.00068.2013.
95. **Alexandre MD, Lu Q, Chen YH.** Overexpression of claudin-7 decreases the paracellular Cl⁻ conductance and increases the paracellular Na⁺ conductance in LLC-PK1 cells. *J Cell Sci* 118: 2683–93, 2005. doi: 10.1242/jcs.02406.